

Geometric Learning and Filtering in Finance

ANASTASIS KRATSIOS* CODY B. HYNDMAN*

December 14, 2024

Abstract

We develop a method for incorporating relevant non-Euclidean geometric information into a broad range of classical filtering and statistical or machine learning algorithms. We apply these techniques to approximate the solution of the non-Euclidean filtering problem to arbitrary precision. We then extend the particle filtering algorithm to compute our asymptotic solution to arbitrary precision. Moreover, we find explicit error bounds measuring the discrepancy between our locally triangulated filter and the true theoretical non-Euclidean filter. Our methods are motivated by certain fundamental problems in mathematical finance. In particular we apply these filtering techniques to incorporate the non-Euclidean geometry present in stochastic volatility models and optimal Markowitz portfolios. We also extend Euclidean statistical or machine learning algorithms to non-Euclidean problems by using the local triangulation technique, which we show improves the accuracy of the original algorithm. We apply the local triangulation method to obtain improvements of the (sparse) principal component analysis and the principal geodesic analysis algorithms and show how these improved algorithms can be used to parsimoniously estimate the evolution of the shape of forward-rate curves. While focused on financial applications, the non-Euclidean geometric techniques presented in this paper can be employed to provide improvements to a range of other statistical or machine learning algorithms and may be useful in other areas of application.

Keywords: Stochastic Filtering, non-Euclidean Filtering, Manifold, Particle Filtering, Machine Learning, Manifold Learning, Shape Recognition, Shape Space, Forward-rate Curve, HJM Framework, Stochastic Volatility, Covariance Matrix, Principal Geodesic Analysis, Dimension Reduction, Geometric Improvement, Stochastic Differential Geometry.

Mathematics Subject Classification (2010): 60D05, 60G35, 91G60, 91G80, 91G99, 93E35, 54C56.

*Department of Mathematics and Statistics, Concordia University, 1455 Boulevard de Maisonneuve Ouest, Montréal, Québec, Canada H3G 1M8. emails: anastasis.kratsios@mail.concordia.ca, cody.hyndman@concordia.ca

This research was supported by the Natural Sciences and Engineering Research Council of Canada (NSERC). The authors thank Alina Stancu (Concordia University) for helpful discussions.

1 Introduction

non-Euclidean geometry naturally occurs in certain problems in finance. For example, in [5] short-rate models consistent with finite-dimensional smooth manifolds were characterized. In [32] highly accurate stochastic volatility model estimation methods are derived using heat-kernel expansions of the Riemannian metric associated with a stochastic volatility model. In [16] arbitrage-free factor models for interest rates have been characterized using geometric methods. In [9] an information-geometric technique for yield-curve modeling was developed, which relies on the Bhattacharyya distance developed in [38], by considering certain finite-dimensional manifolds of probability densities. Each of these cases outlines a very different problem in mathematical finance. However, each relies on differential geometry and many rely, more specifically on Riemannian geometry.

Section 2 of this article begins by reviewing some results from Riemannian-Finsler geometry and examples of how this geometry naturally appears in mathematical finance. In particular, we focus on three examples: the geometry of stochastic volatility models, the geometry of optimal Markowitz portfolios, and the evolution of the shape of the forward-rate curve. The geometry of stochastic volatility models is studied extensively in [31]. The geometry of optimal Markowitz portfolios relies on the matrix geometry developed in [6]. The analysis of the shape of the forward-rate curve relies on the geometry of shape space developed in [39] and [10]. These examples provide the motivation for the general methods and results of this paper.

Section 3 develops a general method for incorporating geometric information into a broad range of Euclidean filtering and statistical or machine learning algorithms by locally triangulating the manifold on which the data lies. We then apply these methods, which are inspired by medical imaging and computer vision literature (see [18]) to stochastic filtering and obtain arbitrarily accurate approximations to the solution of the non-Euclidean filtering problem. These solutions are implementable and converge asymptotically to the non-Euclidean filtering problem. Our solution to the non-Euclidean filtering problem differs from those found in the literature in primarily two ways. On the one hand, it provides a computationally feasible alternative to [15] or [51], and on the other hand it provides a rigorous foundation for the ideas explored in [29] or in [52]. Therefore, our approach is, to the best of our knowledge, the first to prove a general (asymptotic) solution to the non-Euclidean filtering problem which is both computationally feasible. We apply the non-Euclidean filtering method to consider improved prediction of stochastic volatility models by exploiting their non-positive curvature geometry described in [31]. Applications of the non-Euclidean filtering method to the prediction of optimal Markowitz portfolios is also discussed.

In Section 4 we extend the local triangulation technique developed in Section 3 to Euclidean statistical or machine learning algorithms. We prove that the new algorithm, incorporating the information present in the problem's non-Euclidean geometry, improves the accuracy of the original Euclidean algorithm. We then apply this theory to extend a sparse version of the non-Euclidean generalization of principal component analysis (PCA), called principal geodesic analysis (PGA), introduced in [19]. We obtain a novel geometric extension of the PCA algorithm, which must perform at least well as the PCA and PGA algorithms. The algorithm further incorporates ideas of the sparse formulation of the PCA algorithm introduced in [23] which relied on the Elastic-Net regularization and LASSO algorithms of [62] and [56], respectively. We then apply these techniques to analyze the evolution of the shape of the forward-rate curve

using the shape theory developed in [39, 10, 42]. Considering the shape of the forward-rate curve is a common heuristic practice amongst bond-market investors. However, to the best of our knowledge, this paper is the first to provide a rigorous geometric foundation and our methods allow for a concrete description of the evolution of the shape of the forward-rate curve and statistical techniques for incorporating this information in empirical models.

Section 5 concluded and an appendix contains the proof of some technical results.

2 Riemannian Geometry in Mathematical Finance

We begin this section by reviewing some Riemannian geometry along with illustrative examples from mathematical finance that serve as the motivation for our general results.

2.1 The Geometry of Markowitz Portfolio

We begin with one of the fundamental problems of mathematical finance, choosing an optimal portfolio of comprised of risky assets and a riskless asset. The classical Markowitz [41] portfolio problem is to maximize the expected (log)-return of a portfolio comprised of D -risky assets S_t^1, \dots, S_t^D subject to a fixed level of risk, measured by the portfolio's variance. The solution of the problem can be obtained by solving the quadratic optimization problem

$$\hat{w}(t) \triangleq \underset{\substack{w \in \mathbb{R}^D \\ \bar{1}^* w = 1}}{\operatorname{argmax}} \left(-t\mu^* w + \frac{w^* \Sigma w}{2} \right). \quad (2.1)$$

In equation (2.1), $\mu \in \mathbb{R}$ is the vector of the log-returns of the risky assets, Σ is the covariance matrix of the log-returns, w is the vector of portfolio weights expressed as the proportion of wealth invested in each risky asset, $\bar{1}$ is the vector with all its components equal to 1, $*$ indicates transpose, and t is a parameter balancing the objectives of maximizing the portfolio return versus minimizing the portfolio variance. It can be shown that the optimal portfolio weights are given by

$$\hat{w}(t) = \frac{\Sigma^{-1} \bar{1}}{\bar{1}^* \Sigma \bar{1}} + t \left(\Sigma^{-1} \mu - \frac{\bar{1}^* \Sigma^{-1} \mu}{\bar{1}^* \Sigma^{-1} \bar{1}} \Sigma^{-1} \bar{1} \right) \quad (2.2)$$

Taking $t = 0$ in equation (2.2) returns the minimum variance portfolio which results from minimizing the portfolio variance subject to the budget constraint $\bar{1}^* = 1$. By adding a risk free asset to the portfolio we derive similar expressions for the market portfolio and the capital market line. For more details on this approach to portfolio theory see [4]. However, for our purposes equation (2.2) is sufficient to explore the geometric structure associated with optimal portfolio problems.

The optimal portfolio of (2.2) is a function of the covariance matrix of the log-returns Σ as well as the expected log-returns μ . If we assume that there is no degenerate correlation amongst these assets then Σ must be a positive definite matrix and Σ^{-1} is also positive definite. Therefore, the optimal portfolio is a function of the positive definite matrix Σ^{-1} and so it comes equipped with the geometry of the collection of positive definite matrices of dimension $D \times D$.

The collection of D -dimensional symmetric positive definite matrices, denoted P_D^+ , has a well studied geometric structure which lies at the intersection of Riemannian geometry and the geometry Lie groups. This geometry has found many applications in mathematical imaging (see [44]), computer vision (see [48]), and signal processing (see [3]). Moreover, connections between this geometry and information theory have been explored in [54], linking it to the Cramer-Rao lower bound. The geometry of the set of non-degenerate covariance matrices has also found many applications in other areas of applied mathematics.

To understand the geometry of P_D^+ , we first recall that a (smooth) manifold is a shape which can be locally interpreted as a smooth deformation of the familiar Euclidean space. Alternatively, as shown in [61], a connected smooth manifold can be viewed as an open subset of \mathbb{R}^N , for a sufficiently large integer N . To each point p on any manifold \mathcal{M} there is an associated vector space lying tangent to it, called the tangent space, which is typically denoted by $T_p(\mathcal{M})$. The tangent space generalizes the familiar tangent lines from ordinary calculus and is used to model derivatives on \mathcal{M} (see [60] for more details).

As noted in [6], the tangent space on P_D^+ can be associated with the set of $D \times D$ -symmetric matrices $(a_{i,j})_{i,j=1}^D$, which are characterized by their upper-triangular entries $(a_{i,j})_{i,j=1, i \geq j}^D$. We may associate these entries to the Euclidean space \mathbb{R}^d , for $d = D(D+1)/2$, using the lexicographic order on the multi-indexes (i, j) . Define the symmetric-vectorization of an element of P_D^+ by the map

$$\begin{aligned} \text{vect}^S : P_D^+ &\rightarrow \mathbb{R}^d \\ \Sigma &\mapsto (x_1, \dots, x_d) \end{aligned} \tag{2.3}$$

where $\Sigma = (a_{i,j})_{i,j=1, i \geq j}^D$ and

$$\begin{aligned} x_1 &= a_{1,1}, & x_2 &= a_{1,2}, & \dots, & x_D &= a_{1,D} \\ x_{D+1} &= a_{2,2}, & \dots, & x_{2D-1} &= a_{2,D} \\ &\ddots & & & \vdots & & \\ x_d &= a_{d,d}. \end{aligned}$$

Remark 2.1. *The mapping described in equation (2.3) will be called symmetric-vectorization and the vector x will be denoted by $\text{vect}^S(a_{i,j})$. We reserve the term vectorization for the same procedure as outlined in equation (2.3), but with all the matrix's entries being used. Note vectorization would result in redundant entries when the matrix is symmetric, as is the case above, making symmetric vectorization a natural choice.*

Counting the entries in (x_1, \dots, x_d) , we may conclude that the dimension d of the tangent space of $T_p(\mathcal{M})$ is equal to $d \triangleq D(D+1)/2 \leq D^2$, where the inequality corresponds to the dimension of the set of $D \times D$ -matrices. Therefore, the first immediate benefit to working intrinsically to the manifold P_D^+ , rather than treating any covariance matrix as an arbitrary $D \times D$ matrix, is the immediate dimension reduction from D to d . Moreover, since no approximation was made when considering P_D^+ intrinsically rather than embedded in \mathbb{R}^{D^2} this dimension reduction is lossless and presents a strict reduction of the problem's size when $D > 1$.

Further structure can be built onto a smooth manifold by associating an infinitesimal notion of length at each point. This is typically achieved by associating to each tangent space $T_p(\mathcal{M})$

on \mathcal{M} a family of sufficiently well-behaved norms $F(p, \cdot)$ varying smoothly along \mathcal{M} . These are called (reversible-) Finsler functions (see [2] for more details on Finsler-Riemannian geometry). This construction is known as a (reversible)-Finsler manifold. A Finsler manifold for which each norm is induced by an inner-product is called a Riemannian manifold (see [2]). In the Riemannian case, these smoothly-varying inner-products are denoted by g and are called Riemannian metric (tensors). The geodesic distance d between any two points on \mathcal{M} can then be defined by measuring the length of a shortest curve joining them according to this infinitesimal notion of distance.

Similar to a line in \mathbb{R}^d , a curve in \mathcal{M} whose length realizes this minimal distance, if it exists, is called a *geodesic* emanating from p with initial velocity v and it must satisfy the following initial value problem (IVP)

$$\begin{aligned} \frac{d^2\gamma^\lambda}{dt^2} + \Gamma_{\mu\nu}^\lambda \frac{d\gamma^\mu}{dt} \frac{d\gamma^\nu}{dt} &= 0, \\ \gamma(0) &= p \\ \dot{\gamma}(0) &= v. \end{aligned} \tag{2.4}$$

In equation (2.4), $\gamma^\mu = x^\mu \circ \gamma(t)$ are the coordinates of the curve γ and $\Gamma_{\mu\nu}^\lambda$ are the Christoffel symbols of the connection ∇ on \mathcal{M} (see [37] for more details) compare the curvature of the Finsler manifold to that of Euclidean space. This geodesic will be denoted by $\gamma_{p,v}$ and equation (2.4) is referred to as the geodesic equation on (\mathcal{M}, ∇) .

Following [6], the geodesic distance on P_D^+ , which we denote by d^+ , between a point Σ in P_D^+ and the identity matrix I is defined to be

$$d^+(\Sigma, I) \triangleq \|\log(\Sigma)\|_F, \tag{2.5}$$

where \log is the matrix logarithm and $\| - \|_F$ denotes the Frobenius norm. Using the multiplicative structure of P_D^+ this distance may be uniquely translated to any other pair of points Σ_1, Σ_2 on P_D^+ through the use of matrix multiplication. Explicitly this distance formula is

$$d^+(\Sigma_1, \Sigma_2) \triangleq \|\log(\Sigma_2^{-1/2} \Sigma_1 \Sigma_2^{-1/2})\|_F. \tag{2.6}$$

The distance in a complete Finsler manifold can be characterized by its geodesics which exist and uniquely join any two points. Hence on a complete Finsler manifold, equation (2.4) puts geodesics in a one-to-one correspondence with vectors in \mathbb{R}^d corresponding to the initial velocity of the geodesic. In the particular case of P_D^+ the geodesics emanating from the identity matrix I for the distance d^+ are of the form

$$\gamma_{[I,v]}(t) \triangleq \exp(tv).$$

Translating about P_D^+ through the matrix multiplication, a geodesic with velocity v , emanating from a point Σ in P_D^+ is of the form

$$\gamma_{[\Sigma,v]}(t) \triangleq \sqrt{\Sigma} \exp\left(t\sqrt{\Sigma}^{-1} v \sqrt{\Sigma}^{-1}\right) \sqrt{\Sigma}. \tag{2.7}$$

The map taking a velocity vector in the tangent space above a p to the evaluation of the geodesic $\gamma_{[\Sigma,v]}(t)$ at time $t = 1$ is known as the Riemannian-Finsler exponential map and is

denoted by $Exp_p(\cdot)$. Its maximal domain of definition is known as the normal coordinate patch about p . This inverse can be interpreted as associating to each point q , in the normal coordinates about p , to the velocity and direction needed for a geodesic travelling from p to reach q at time 1 (see [2] for more details). This inverse of the Exp_p map is called the Riemannian-Finsler Log map. In the case of P_D^+ , since its elements are positive-definite matrices, they must have strictly positive-eigenvalues (see [20]), in which case the matrix exponential map exp has a unique inverse called the principal logarithm, log , as in [34, Theorem 1.31]. This important algebraic information is encoded into the Riemannian-Finsler log map of P_D^+ which can be written as

$$Log_{\Sigma_1}(\Sigma_2) \triangleq \sqrt{\Sigma_1} \log \left(\sqrt{\Sigma_1}^{-1} \Sigma_2 \sqrt{\Sigma_1}^{-1} \right) \sqrt{\Sigma_1}. \quad (2.8)$$

It can additionally be shown that this is the unique geometry which yields a metric invariant under both left and right matrix multiplication, (see [6]), making d^+ the most natural algebraic as well as geometric choice of a metric on P_D^+ .

Besides distance, one of the most fundamental concepts in Riemannian-Finsler geometry, is the comparison of the angles between geodesic curves to their Euclidean counterparts in normal coordinates. For example, when the manifold is Euclidean space then the sectional curvature is 0. In contrast, it is shown in [43] that the manifold P_D^+ of positive definite matrices has negative curvature. This means that the angles between geodesic curves on P_D^+ are strictly smaller than their corresponding Euclidean lines in the tangent space which is identified with Euclidean space.

In Section 3 we will be interested in the case where the Riemannian metric is time-dependent. We may consider any Riemannian manifold (\mathcal{M}, g_t) with time-dependent metric as a sub-manifold of some suitably high-dimensional Euclidean space \mathbb{R}^D by the Nash embedding theorem of [47]. Riemannian manifolds (\mathcal{M}, g_t) with time-dependent Riemannian metrics are called flows (see [45] for details). Hence, we make the following definition.

Definition 2.2 (Cartan-Hadamard-Finsler Flow). *Let \mathcal{M} be a smooth geodesically complete Finsler (resp. Riemannian) manifold and let $\{F_t\}_{t \in [0, \infty)}$ be a family of Finsler functions on \mathcal{M} such that*

- (i) *The map $t \mapsto F_t$ is continuously differentiable on \mathcal{M} ,*
- (ii) *For every $t \in [0, \infty)$ the Finsler manifold (\mathcal{M}, F_t) has non-positive sectional curvature everywhere,*
- (iii) *\mathcal{M} is simply-connected.*

The pair (\mathcal{M}, F_t) is called a Cartan-Hadamard-Finsler flow. In the case where the Finsler manifold is Riemannian, we denote the Cartan-Hadamard-Finsler flow by (\mathcal{M}, g_t) and refer to it simply as a Cartan-Hadamard flow. Moreover, if g_t is constant in t , we will say that (\mathcal{M}, g_t) is a Cartan-Hadamard manifold and write (\mathcal{M}, g) .

Additional properties of Cartan-Hadamard manifolds are that they are complete as a metric space and that they are geodesically complete. That is, any two points can be joined unambiguously by a unique geodesic of minimal distance. Furthermore, the normal coordinates about any point are defined on the entire manifold. All three of these useful properties are a consequence

of the main theorem of [35]. We now explore two classes of finance problems which hide a Cartan-Hadamard flow geometry.

Returning to the portfolio optimization problem of equation (2.1) we note that equation (2.2) characterizes an optimal portfolio in terms of the mean and covariance matrix of the risky asset log-returns. Assuming non-degeneracy of the covariance matrix this means that any optimal portfolio, as in equation (2.2), defines a bijection with points in the manifold $P_D^+ \times \mathbb{R}^D$ via the map

$$w(\Sigma, \mu) \mapsto \frac{\Sigma^{-1}\bar{1}}{\bar{1}^*\Sigma\bar{1}} + t \left(\Sigma^{-1}\mu - \frac{\bar{1}^*\Sigma^{-1}\mu}{\bar{1}^*\Sigma^{-1}\bar{1}} \Sigma^{-1}\bar{1} \right). \quad (2.9)$$

Endow $P_D^+ \times \mathbb{R}^D$ with the Riemannian product metric. We will require the following standard result, which we take the time to review.

Lemma 2.3. *Let (\mathcal{M}, g^M) and (\mathcal{N}, g^N) and let γ_M and γ_N be geodesics on (\mathcal{M}, g^M) and (\mathcal{N}, g^N) . Then (γ_M, γ_N) is a geodesic on the product Riemannian manifold $(\mathcal{M} \times \mathcal{N}, g^{M \times N})$.*

Proof. Let ∇^M and ∇^N be the Levi-Civita connections corresponding to the Riemannian metrics g^M and g^N , respectively. The Levi-Civita connection $\nabla^{M \times N}$ on the product manifold $(\mathcal{M} \times \mathcal{N}, g^{M \times N})$ is defined as

$$\nabla^M + \nabla^N,$$

and the tangent space of $\mathcal{M} \times \mathcal{N}$ at any point is the direct sum of the tangent spaces on \mathcal{M} and \mathcal{N} . Therefore

$$\nabla^{M \times N}(\gamma_M, \gamma_N) = \nabla^M \dot{\gamma}_M + \nabla^N \dot{\gamma}_N = 0 + 0 = 0.$$

For more details on the Levi-Civita connection see [37]. □

Lemma 2.3 implies that the Riemannian exponential and log maps on $(P_D^+ \times \mathbb{R}^D, g^M)$ must be of the form

$$\begin{aligned} \text{Exp}(w(\Sigma, \mu), (v_1, v_2)) &= w \left(\sqrt{\Sigma} \exp \left(t \sqrt{\Sigma}^{-1} v_1 \sqrt{\Sigma}^{-1} \right) \sqrt{\Sigma}, \mu_1 + v_2 \right) \\ \text{Log}(w(\Sigma_1, \mu_1), w(\Sigma_2, \mu_2)) &= w \left(\sqrt{\Sigma_1} \log \left(\sqrt{\Sigma_1}^{-1} \Sigma_2 \sqrt{\Sigma_1}^{-1} \right) \sqrt{\Sigma_1}, \mu_2 - \mu_1 \right), \end{aligned} \quad (2.10)$$

where v_1 is in the tangent space of Σ , v_2 is in the tangent space of μ and (v_1, v_2) is in the tangent space of the product $w(\Sigma_1, \mu_2)$. Similarly, it implies that since both (P_D^+, g^+) and (\mathbb{R}^D, g_E) have non-positive curvature, are geodesically complete and are simply connected then it can be shown that their product Riemannian manifold must also share these properties (see [37] for more details on products of Riemannian manifolds). Therefore $(P_D^+ \times \mathbb{R}^D, g^M)$ must also be a Cartan-Hadamard manifold. Moreover, the metric d^{Mrk} induced by the product Riemannian metric g^{Mrk} , is the product metric and therefore must be of the form

$$\begin{aligned} d^{Mrk}(w(\Sigma_1, \mu_1), w(\Sigma_2, \mu_2)) &= \sqrt{d^M(\Sigma_1, \Sigma_2)^2 + d_E(\mu_1, \mu_2)^2} \\ &= \sqrt{\|\log(\Sigma_2^{-1/2} \Sigma_1 \Sigma_2^{-1/2})\|_F^2 + \|\mu_1 - \mu_2\|^2}. \end{aligned} \quad (2.11)$$

where v_1 is in the tangent space of Σ , v_2 is in the tangent space of μ and (v_1, v_2) is in the tangent space of the product $w(\Sigma_1, \mu_2)$. This leads to the following definition.

Definition 2.4 (Markowitz Manifold). *The collection of optimal portfolios, identified with the Cartan-Hadamard manifold $(P_D^+ \times \mathbb{R}^D, g_{Mrk})$ under equation (2.9) is called the Markowitz manifold.*

We next present another example of the Cartan-Hadamard geometry in mathematical finance, the geometry present in stochastic volatility models.

2.2 The Geometry of Stochastic Volatility Models

Every stochastic volatility model (SVM) carries with it a natural geometry which we describe following [31]. Let f_t be the price of a forward (rate or price) with maturity T and let a_t be the instantaneous stochastic volatility of f_t . Since a_t is not directly observable there may exist more than one equivalent σ -martingale measure (E σ MM). We focus on the forward-measure \mathbb{P}^T , associated with the zero-coupon bond maturing at time T as numéraire, under which f_t follows the one-dimensional dynamics

$$\begin{aligned} f_t &= f_0 + \int_0^t a_t C(t, f_t) dW_t, \\ a_t &= a_0 + \int_0^t b(t, a_t) dt + \int_0^t \sigma(t, a_t) dZ_t \\ [W, Z]_t &= \rho_0 + \int_0^t \rho_t dt, \end{aligned} \tag{2.12}$$

where C, b, σ are smooth functions such that the process f_t is defined for all time $0 \leq t \leq T$.

Example 2.5 (Heston Model). *The Heston [33] stochastic volatility model, is popular due to the mean reverting property of the volatility process a_t and the flexibility its relatively simple parameterization. The Heston model is the SVM defined by the following dynamics*

$$\begin{aligned} df_t &= a_t f_t dW_t^1 \\ da_t^2 &= \lambda(\nu - a_t^2) dt + \zeta a_t dW_t^2 \\ dW_t dZ_t &= \rho dt. \end{aligned} \tag{2.13}$$

Example 2.6 (SABR Model). *An alternative to the Heston model is the stochastic alpha beta rho, or SABR, stochastic volatility model of [26, 27]. The SABR model is popular due to its simplicity and the accurate forecasts for interest rate futures which it provides. The SABR model is defined by*

$$\begin{aligned} df_t &= \alpha_t f_t^\beta dW_t^1; f_0 = f \\ d\alpha_t &= \nu \alpha_t dW_t^2; \alpha_0 = \alpha, \end{aligned} \tag{2.14}$$

where f is a forward-rate, σ is a non-negative volatility parameter, W_t^1 and W_t^2 are correlated Brownian motions with correlation matrix given by

$$Q \triangleq \begin{pmatrix} 1 & 0 \\ \rho & \sqrt{1 - \rho^2} \end{pmatrix}.$$

Here α is the vol of the vol, β is a leverage parameter which is also non-negative and the correlation coefficient is $\rho \in [-1, 1]$. The parameter α determines the at-the-money forward

volatility, the parameter β controls the effect of the stochastic volatility on the forward-rate curve and ν affects the convexity, that is the vol of the vol (see [53] for more details).

In commodity markets it can be observed that the prices become more volatile as they increase. In contrast, in equity markets the opposite empirical behaviour is observed as discussed in [21]. Since the model can handle the a wide range of different markets, the forward-rate is intentionally left general. Therefore f_t can represent the forward-rate on a zero-coupon bond, a LIBOR forward-rate, forward swap rate or possibly something more exotic (see, [25]).

In two dimensions, following [31], it can be shown that put-call parity is preserved if and only if f_t is a martingale, which is in turn equivalent to requiring that instantaneous volatility process ξ_t defined by

$$\xi_t \triangleq \frac{C(t, f_t) a_t}{f_t},$$

does not explode under the measure \mathbb{P}^f associated with the forward as numéraire. Under the forward measure \mathbb{P}^T the dynamics of ξ_t can be written as

$$\begin{aligned} \xi_t = & \xi_0 + \int_0^t a_s C(s, f_s) \frac{\partial C(s, f_s)}{\partial f} dW_s + \int_0^t \frac{C(s, f_s)}{f_s} \sigma(s, a_s) dZ_s \\ & + \int_0^t \left(\frac{C(s, f_s)}{f_s} b(s, a_s) + \frac{\partial C(s, f_s)}{\partial f} C(s, f_s) a_s \rho_s \sigma(s, a_s) + \frac{a_s^3}{2} C(s, f_s)^2 \frac{\partial^2 C(s, f_s)}{\partial f^2} \right) ds. \end{aligned} \quad (2.15)$$

The Riemannian metric to associated with an SVM, as presented in [31, equation 4.54], is a ratio of the correlation over the covariance of the diffusion process; the intuition being that under this metric the process behaves like a Brownian motion on \mathbb{R}^2 . An interpretation of the central theorem of [58] is that if particles are diffused on \mathbb{R}^2 according to a Brownian motion, then the most distant ones from their originating point correspond to ones that travelled in the straightest line. Therefore, this Riemannian metric compares geodesics of an SVM to the corresponding straight lines in the tangent space. Hence, this provides an intrinsic linearization of the problem.

In detail, the explicit change of coordinates needed is

$$\begin{aligned} x & \triangleq \int_{f_0}^f \frac{df'}{C(f')} - \rho \int_{\cdot}^a \frac{u}{\sigma(u)} du \\ y & \triangleq \sqrt{1 - \rho^2} \int_{\cdot}^a \frac{u}{\sigma(u)} du. \end{aligned} \quad (2.16)$$

Under this change of coordinates the Riemannian metric corresponding to the SVM becomes

$$\begin{aligned} ds^2 & = e^{\phi(y)} (x^2 + y^2) \\ \phi(y) & = \ln(2) - \ln(a(y)^2(1 - \rho^2)). \end{aligned} \quad (2.17)$$

The geodesic distance under this Riemannian metric, using the coordinate system described by equation (2.16), is given by

$$\begin{aligned} d((x_1, y_1), (x_2, y_2)) & = \int_{y_1}^{y_2} \frac{e^{\phi(y')} dy'}{\sqrt{e^{\phi(y')} - C^2}} \\ x_1 - x_2 & \triangleq \int_{y_1}^{y_2} \frac{C}{\sqrt{e^{\phi(y')} - C^2}} dy'. \end{aligned} \quad (2.18)$$

A fundamental result from the theory of 2-dimensional Riemannian manifolds is that every Riemannian metric on a Riemannian manifold of dimension 2, called a Riemannian surface, is conformally equivalent to either \mathbb{R}^2 , the sphere, or the upper-half plane under the hyperbolic metric. Since the sphere is compact while volatility can become arbitrarily large, the Riemannian metric associated to any one-dimensional SVM is either conformally equivalent to the Euclidean or hyperbolic metric. The former is a space of zero sectional-curvature and the latter is a space of constant negative sectional curvature. We may conclude that the Riemannian manifold associated with any SVM has non-positive curvature. This makes it reasonable to assume that the associated Riemannian geometry of (f_t, a_t) is that of a Cartan-Hadamard manifold. In particular, the sectional curvature¹ R is given by

$$R = \frac{-e^{\phi(y)} \frac{\partial^2 e^{\phi(y)}}{\partial y^2} - \left(\frac{\partial e^{\phi(y)}}{\partial y} \right)^2}{e^{3\phi(y)}} = \frac{\sigma(a)^2}{2a} \left(\frac{\sigma'(a)}{\sigma(a)} - \frac{2}{a} \right). \quad (2.19)$$

2.3 Shape of the Forward-Rate Curve

We next consider the geometry associated to the evolution of the shape of the forward-rate curve. This is an example of Riemannian geometry which need not be of non-positive sectional curvature. In fact many formulations of the theory of shape, such as [39], consider Riemannian manifolds with strictly positive curvature.

The Heath-Jarrow-Morton [30] (HJM) modeling framework prices a zero-coupon bond as a function of the entire forward-rate curve (FRC). The FRC is then the object being directly modelled instead of the bond price. The price of a zero-coupon bond $B(t, T)$ with maturity time $T \geq t$ is modelled as a function of all the FRC $f(t, T)$ as

$$B(t, T) \triangleq e^{- \int_t^T f(t, u) du}.$$

where $T \rightarrow f(t, T)$ is the instantaneous forward-rate curve at time t . The evolution of the FRC is typically described point-wise using the available data. Unfortunately this is not descriptive of the shape of the FRC as whole object, itself. Heuristically, the shape of the FRC can be used when trading, for example, long positions are desirable when the FRC has an overall increasing shape slope and short positions when the FRC has an overall downwards sloping shape. Likewise, more complex yet similar shape-based heuristics are often made use of in a variety of ways in the empirical technical analysis literature (see [46] for example).

Instead of estimating the FRC using point-wise techniques we appeal to shape theory (see [39]) that has been applied extensively in the imaging and manifold learning literature. Following [42], the set of all smooth, closed planar curves with non-vanishing tangent vectors can be viewed as the infinite-dimensional manifold of maps from the circle S^1 into \mathbb{R}^2 . We denote this space by $\text{Imm}(S^1; \mathbb{R}^2)$ and call it the space of immersed planar curves. This smooth manifold can be endowed with a family of Riemannian metrics G^n defined on the tangent space at any $c \in \text{Imm}(S^1; \mathbb{R}^2)$ by

$$G_c^n(h, k) \triangleq \int_0^{2\pi} \sum_{j=0}^n \langle D_s^j h, D_s^j k \rangle ds, \quad (2.20)$$

¹We are using the fact that in two dimensions the scalar and sectional curvatures differ by a factor of 2.

where a_j are non-negative real numbers such that $a_0, a_n \neq 0$, h, k are vector fields along c , $ds = |c'|d\theta$ is the arc-length measure, $D_s \triangleq \partial_\theta / \|c'\|$ denotes the arc-length derivative operator, $v \triangleq c'/\|c'\|$ is the unit tangent vector and $\langle \cdot, \cdot \rangle$ is the Euclidean inner-product. In [10] it is shown that G_c^n defines a geodesically complete Riemannian metric on $\text{Imm}(S^1; \mathbb{R}^2)$ for $n \geq 2$. Moreover [10, Theorem 2] showed that the initial value problem (IVP) describing a geodesic in $(\text{Imm}(S^1; \mathbb{R}^2), G^n(,))$ is given explicitly by

$$\begin{aligned} \partial_t \left(\sum_{j=0}^n (-1)^j |c'| D_s^{2j} c_t \right) &= -\frac{a_0}{2} |c'| D_s (\langle c_t, c_t \rangle v) + \sum_{k=1}^n \sum_{j=1}^{2k-1} (-1)^{k+j} \frac{a_k}{2} |c'| D_s (\langle D_s^{2k-j} c_t, D_s^j c_t \rangle v) \\ c_0 &= u; \quad c'_0 = c, \end{aligned} \quad (2.21)$$

where $c \in \text{Imm}(S^1; \mathbb{R}^2)$ and u is a tangent vector in $\text{Imm}(S^1; \mathbb{R}^2)$.

The forward-rate curve $T \rightarrow f(t, T)$ is a planar curve which is typically assumed to be smooth in T . However, by definition, it is never closed and so is can never be an element of $\text{Imm}(S^1; \mathbb{R}^2)$. This issue can be surmounted through the following transformation.

Definition 2.7 (Loop Transform). *Let f be a curve from $[0, T]$ to \mathbb{R}^+ . The (closed) loop $l(\theta) : [0, 2\pi) \rightarrow \mathbb{R}^2$ induced by the curve f is defined to be $l_f(\theta)$*

$$\begin{aligned} l_f : [0, 2\pi) &\rightarrow \mathbb{C} \\ \theta &\mapsto \left(f\left(\frac{\theta 2\pi}{T}\right) - \frac{\theta(f(T) - f(0))}{T} \right) e^{i\theta} \end{aligned} \quad (2.22)$$

where the image of l_f in \mathbb{C} and is identified with \mathbb{R}^2 . We will call $f \mapsto l_f$ the loop transform of f .

Lemma 2.8. *Denote the modulus on \mathbb{C} by $|\cdot|$. The map \tilde{l}_f defined on any non-self intersecting element $l(\theta)$ of $\text{Imm}(S^1; \mathbb{R}^2)$ as*

$$\tilde{l}(l)(t) \triangleq |l\left(\frac{tT}{2\pi}\right)| + \left(\frac{t(f(T) - f(0))}{2\pi}\right), \quad (2.23)$$

is the inverse of l_f , provided that f is non-negative, smooth and takes values in \mathbb{R} .

Proof. Let f be a non-negative and smooth real-valued function. Then

$$\begin{aligned} \tilde{l}(l_f)(t) &= \tilde{l}\left(\left(f\left(\frac{t2\pi}{T}\right) - \frac{t(f(T) - f(0))}{T}\right) e^{it}\right) \\ &= \left| \left(f\left(\frac{tT2\pi}{T2\pi}\right) - \frac{\frac{tT}{2\pi}(f(T) - f(0))}{T}\right) e^{it\frac{tT}{2\pi}} \right| + \left(\frac{t(f(T) - f(0))}{2\pi}\right) \\ &= \left(f(t) - \frac{tT(f(T) - f(0))}{T2\pi}\right) + \left(\frac{t(f(T) - f(0))}{2\pi}\right) \\ &= f(t). \end{aligned}$$

The other composition follows similarly. \square

The correspondence between non-negative planar curves and non-intersecting complex loops, provided by Lemma 2.8, may be interpreted as providing a correspondence between the classical description of the FRC of [30] and a description of the evolution of the shape of the FRC. Hence, Lemma 2.8 allows us to model the evolution of the shape of the FRC, instead of looking at it simply from the point-wise vantage-point. Therefore, our approach is not to model the FRC directly, but rather by modeling $l(t, \theta)$ through a description of its linearized dynamics in tangent space $T_{l(0, \theta)}(\mathcal{M})$ using the Riemannian Log map, which can always be accomplished locally for complete Riemannian manifolds. We then return to the shape space, using the Riemannian Exp map, and use the transformation provided by Lemma 2.8 to obtain the FRC.

Definition 2.9 (Shape Parameterization). *Let the linearization of the shape of the FRC be defined as a family of \mathbb{R}^D valued stochastic processes $\{X_t(\theta)\}_{\theta \in [0, 2\pi]}$, let f_t^T be an \mathbb{R} -valued stochastic process modeling the evolution of the last observed data on the FRC, which is used to close the loop, and let f be the observed forward-rate curve at time 0. The shape of the forward rate curve is defined to be the Imm $(S^1; \mathbb{R}^2) \times \mathbb{R}$ -valued semi-martingale $(l(t, \theta), f_t^T)$ where $l(t, \theta)$ is defined by*

$$l(0, \theta) \triangleq \begin{cases} l_f & t = 0 \\ \text{Exp}(l(0, \theta), X_t(\theta)) & t > 0 \end{cases}.$$

We require that $\{X_t(\theta)\}_{\theta \in [0, 2\pi]}$ and f_t^T solve the SDEs

$$\begin{aligned} dX_t(\theta) &= \mu(t, \theta, X_t(\theta))dt + \sigma(t, \theta, X_t(\theta))dW_t^X; X_0(\theta) = 0 \\ df_t^T &= \alpha(t, f_t^T)dt + \beta(t, f_t^T)dW_t^f; f_0^T = f(T) \end{aligned} \tag{2.24}$$

here that $\mu, \alpha, \beta, \sigma$ are $\mathbb{R}, \mathbb{R}, \mathbb{R}^n$ and \mathbb{R}^d -valued processes, respectively; here W_t^X and W_t^f are 1 and d -dimensional independent Brownian motions, respectively. Furthermore, we require that following assumptions are met

- (i) The maps $\{\theta \mapsto X_t(\theta)\}_{t \in [0, \infty)}$ are continuously differentiable,
- (ii) $\mu, \sigma, \alpha, \beta$ are $\sigma(W_\star, B_\star)_t \otimes \mathfrak{B}_t$ -progressively measurable, for every $\theta \in [0, 2\pi]$,
- (iii) $\max \left\{ \int_0^T \int_0^{2\pi} \int_{\mathbb{R}^d} |\mu(s, \theta, x)| ds d\theta dx, \int_0^T \int_{\mathbb{R}} |\alpha(s, x)| ds dx \right\} < \infty$,
- (iv) $\max \left\{ \sup_{s, \theta \leq 2\pi; x \in \mathbb{R}^d} \|\sigma(s, \theta, x)\|, \sup_{s, \theta \leq 2\pi; x \in \mathbb{R}^d} \|\beta(s, x)\| \right\} < \infty$,

Using the correspondence between provided by Lemma 2.8, the shape of the FRC may be used to recreate the FRC $f(t, T)$ of the HJM modeling framework by defining $f(t, T)$ to be

$$f(t, T) \triangleq \tilde{l}(t, \theta) = \left| l \left(t, \frac{\theta T}{2\pi} \right) \right| + \left(\frac{\theta (f_t^T - l(t, 0))}{2\pi} \right). \tag{2.25}$$

Proposition 2.10. *Let $l(t, \theta)$ be the shape of the forward-rate curve and define the forward-rate curve $f(t, T)$ as in Equation (2.25). Then the price of a zero-coupon bond $B(t, T)$ may be expressed as*

$$B(t, T) = \exp \left(- \int_t^T \left| l \left(t, \frac{\theta T}{2\pi} \right) \right| + \left(\frac{\theta (f_t^T - l(t, 0))}{2\pi} \right) d\theta \right). \tag{2.26}$$

Proof. The HJM modeling framework prices a zero-coupon bond by

$$B(t, T) = e^{-\int_t^T f(t, u) du}. \quad (2.27)$$

Using correspondence between the shape of the FRC and $f(t, T)$ itself provided by Equation (2.25) the process $B(t, T)$ in Equation (2.27) may be described as in Equation (2.26). \square

Remark 2.11. *The advantage of using the shape of the forward-rate curve over the forward-rate curve itself is that the evolution of the geometry of the curve of forward interest rate can be directly modelled as a whole.*

Each of the three examples provided in this section demonstrates aspects of non-Euclidean geometry present in fundamental areas of finance: portfolio theory, volatility modeling; and term-structure modeling. Our objective in the remainder of the paper is to exploit the inherent non-Euclidean geometry of each of these examples to improve the performance of classical Euclidean algorithms that ignore this structure.

3 Locally Triangulated Algorithms and non-Euclidean Filtering

In this section we extend any Euclidean filtering and statistical or machine learning algorithms to the Finsler setting through the use of a local triangulation of the manifold. That is, we locally approximate the manifold by a piecewise linear sub-manifold in a way which maps geodesics to lines. The Euclidean algorithm is then applied in the tangent space of a point x_Δ in \mathcal{M} . Lastly, the resulting outputs are returned to \mathcal{M} via the normal coordinate patch about the point x_Δ . Figure 1 provides a simple illustration of this procedure when \mathcal{M} is a sphere.

Locally Triangulation of an Algorithm

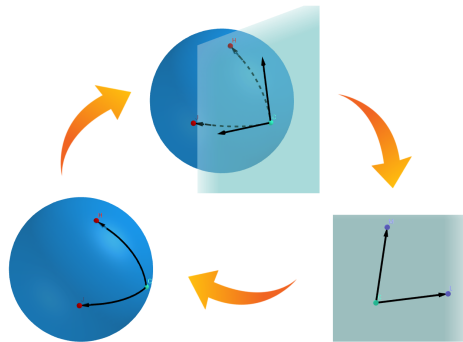


Figure 1: The \mathcal{M} -valued data $\{x_i\}_{i=1}^N$ is linearized by first selecting a reference point x_Δ on \mathcal{M} , then considering the \mathbb{R}^d -valued data $\{\text{Log}(x_i, x_\Delta)\}_{i=1}^N$, performing the Euclidean algorithm A therein and subsequently returning the points onto \mathcal{M} via the exponential map.

The approximate principal geodesic analysis (PGA) of [19], the geodesic regression models of [17], the geometric unscented Kalman filter of [29], and the geometric GARCH models for covariance matrices of [28] all provide particular cases of this general method. In this section we are primarily interested in the general theory, and specifically how this technique can be

used to asymptotically solve the non-Euclidean filtering problem for data taking values in a Cartan-Hadamard flow and its applications in mathematical finance. We now formalize this general method before moving on to its application to solve the non-Euclidean stochastic filtering problem in a computable manner.

Definition 3.1 (Local Triangulation). *Let $\{(t_i, x_i)\}_{i=1}^N$ be data on the $d+1$ -dimensional Finsler flow (\mathcal{M}, g) , x_Δ be a point on \mathcal{M} , and A be an algorithm with inputs being points on \mathbb{R}^d and outputs being points on \mathbb{R}^d . The Local Triangulation of A on (\mathcal{M}, g) is defined by Algorithm 3.1:*

Algorithm 3.1: Local Triangulation

Data: The (\mathcal{M}, F_t) -valued data $\{(t_i, x_i)\}_{i=1}^N$
Result: The (\mathcal{M}, F_t) -valued data $\{y_i\}_{i=1}^N$

```

if There exists  $x_i \in \mathcal{M} - \text{Cut}^{F_{t_i}}(x_\Delta)$  then
    (i) for  $i \in \{1, \dots, N\}$  do
        if  $x_i \in \mathcal{M} - \text{Cut}^{F_{t_i}}(x_\Delta)$  then
            | Set  $\tilde{x}_i \triangleq x_i$ ,
        end
    end
    (ii) Define  $\tilde{N}$  to be  $\#(\{\tilde{x}_i : x_i \in \mathcal{M} - \text{Cut}^{F_{t_i}}(x_\Delta)\})$ ,
    (iii) if  $\tilde{x}_i = x_\Delta$  then
        | Define  $\tilde{y}_i \triangleq \tilde{x}_i$ 
        | else
        | Define  $\tilde{y}_i$  as the  $i^{th}$  element of the set  $A(\{\text{Log}^{F_{t_i}}(\tilde{x}_i, x_\Delta)\})$ ,
        | end
    (iv) Define  $y_i$  as  $\text{Exp}^{F_{t_i}}(\tilde{y}_i, x_\Delta)$ ,
    (v) Define  $M \triangleq \#A(\{\text{Log}^{F_{t_i}}(\tilde{x}_i, x_\Delta)\})$ .
else
    (i) Define  $y_1 \triangleq x_\Delta$ ,
    (ii) Define  $M \triangleq 1$ .
end
Return the set  $\{y_i\}_{i=1}^M$ .
```

We will denote the local triangulation of A on (\mathcal{M}, F_t) by $A_{(\mathcal{M}, F_t)}^{x_\Delta}$. In the Riemannian case, we denote it by $A_{(\mathcal{M}, g)}^{x_\Delta}$.

Remark 3.2. The set $\text{Cut}^{F_t}(x)$ in Definition 3.1 denotes the complement of the normal-coordinate path about x in \mathcal{M} with respect to the Finsler function F_t . This set, called the

cut-locus about x , is inconsequential since it can be shown to be of measure 0 (for a proof in the Riemannian case see [37]).

Remark 3.3. Step 3 of Algorithm 3.1 is only required in the general Finsler case since when the Finsler function is not Riemannian it may happen that the tangent space is missing the 0 vector.

3.1 Locally Triangulated Filtering and Estimation of SVMs and Markowitz Portfolios

We begin by introducing an objective function for the stochastic filtering problem which, unlike the classical Euclidean least-squares objective function, encodes information about the geometry of Markowitz portfolio optimization and stochastic volatility models. However, while these objective functions are more natural they come with additional complexity. Both are new filtering problems and so require new solutions, and a priori computationally more involved than the classical Euclidean objective function.

Example 3.4 (Predicting Optimal Markowitz Portfolios). *The Markowitz portfolio optimization problem outlined in equation (2.1) is a static problem at a particular time. The solution of this problem given by equation (2.2) depends on the expected log-returns μ and the covariance matrix of the log-returns Σ . However, it is well known that these quantities vary over time. We consider using filtering techniques in order to predict the stochastic log-returns and covariance matrix μ_t and Σ_t from the returns of the risky assets.*

A naive stochastic filtering approach would be to first use the identification made in equation (2.2) and then vectorize the matrix Σ_t and describing dynamics for the signal process

$$X_t \triangleq (\mu_t, \text{vect}(\Sigma_t)), \quad (3.1)$$

in terms of the log-returns R_t which play the role of the observation process. The classical filtering problem applied to the Markowitz prediction problem would then seek dynamics for the density of the optional projection of the random variable

$$\underset{Z \in L^2(\mathcal{F}_t)}{\text{arginf}} \mathbb{E} \left[(X_t - Z)^2 \right], \quad (3.2)$$

where \mathcal{F}_t is the σ -field generated by the returns process R_t .

However, the vectorization of the signal process performed in equation (3.1) ignores the natural geometry of the Markowitz manifold described in Section 2.1. Likewise, the Euclidean distance used in defining the objective function of the filtering problem described in equation (3.2) again ignores the natural geodesic distance present in the Riemannian geometry of the Markowitz manifold $(P_D^+ \times \mathbb{R}^D, g_{\text{Mrk}})$.

Therefore, a more natural formulation of the prediction problem for the optimal portfolio using stochastic filtering would first assume that the signal, $\xi_t = w(\mu_t, \Sigma_t)$ is a suitable semi-martingale taking values in $(P_D^+ \times \mathbb{R}^D, g_{\text{Mrk}})$. We model the returns process R_t as a noisy function of ξ_t and the filtering problem would uses the objective function

$$\begin{aligned} \operatorname{arginf}_{Z \in L^2(\mathcal{F}_t)} \mathbb{E} \left[d^{Mrk} (\xi_t, Z)^2 \right] &= \operatorname{arginf}_{Z \in L^2(\mathcal{F}_t)} \left(\mathbb{E} \left[\|\xi_{2,t} - Z_2\|^2 \right] + \mathbb{E} \left[\|\log \left(Z_1^{-1/2} \xi_{1,t} Z_1^{-1/2} \right)\|_F^2 \right] \right) \\ &= \operatorname{arginf}_{Z \in L^2(\mathcal{F}_t)} \left(\mathbb{E} \left[\|\xi_{2,t} - Z_2\|^2 \right] + \mathbb{E} \left[\sum_{i=1}^D \sigma_i(Z_1; \xi_{1,t})^2 \right] \right), \end{aligned} \quad (3.3)$$

Therefore, the objective function of equation (3.2) is replaced with the geometric objective function. In equation (3.3), the quantities $\sigma_i(Z_1; \xi_{1,t})$ denote the singular-values of the matrix $\sigma_i(Z_2; \xi_{1,t}) \log \left(Z_1^{-1/2} \xi_{1,t} Z_1^{-1/2} \right)$.

We may interpret the new geometric objective function described in equation (3.3) as penalizing the Euclidean objective function for the mean by a non-Euclidean penalty weighted by estimates on the singular values of the covariance of the returns, encoded in the first component $\xi_{1,t}$ of the signal process ξ_t .

Example 3.5 (Estimating SVMs). Consider a stochastic volatility model (f_t, a_t) . We have seen that every SVM carries a natural Riemannian geometry through the change of coordinates defined in equation (2.17). Let ξ_t denote the process taking values in this Cartan-Hadamard flow defined by the pair of the price of a forward and its stochastic volatility, denoted by (f_t, α_t) , under the the change of coordinates describe in equation (2.17).

Our goal is to minimize the expected geodesic distance defined in equation (2.18) given the σ -algebra generated by the observable forward-rate price process f_t . That is we wish to minimize,

$$\begin{aligned} \operatorname{arginf}_{Z \in L^2(\mathcal{F}_t; \mathbb{R}^2); Z_1 > 0} \mathbb{E} [d^2((\xi_t), Z)] &= \mathbb{E} \left[\left(\int_{\xi_{2,t}}^{Z_2} \frac{e^{\phi(y')} dy'}{\sqrt{e^{\phi(y')} - C(\xi_t, Z)^2}} \right)^2 \right], \\ \xi_{1,t} - Z_2 &\triangleq \int_{\xi_{1,t}}^{Z_2} \frac{C}{\sqrt{e^{\phi(y')} - C^2}} dy'. \end{aligned} \quad (3.4)$$

where \mathcal{F}_t is the σ -field generated by the forward-rate price process f_t , which can be directly observed. Here $\xi_{i,t}$ and Z_i are the i^{th} -coordinates of the random elements ξ_t and Z , respectively (for $i = 1, 2$). Note that ϕ is a function of the stochastic volatility process α_t , and therefore is a function of ξ_t .

In principle, equation (3.4) represents an objective function which encodes more information about the problem than the classical least-squares objective function used in the Euclidean filtering problem. The issue however, is that it is clearly vastly more complicated than the least-squares objective function. The remainder of this section discusses how to asymptotically overcome this computational barrier with the proper choice of a sequence of Euclidean objective functions.

An \mathcal{M} -valued semi-martingale² ξ_t is defined to be an \mathbb{R}^D -valued semi-martingale such that \mathbb{P} -a.s. the paths of ξ_t are entirely contained within \mathcal{M} . In the case where the semi-martingale's paths are required to be \mathbb{P} -a.s. continuous there is an intuitive description of ξ_t . In [14]

² Many definitions require an \mathcal{M} -valued semi-martingale to have \mathbb{P} -a.s. continuous paths. We do not make this assumption unless explicitly stated otherwise.

and in [36], the evolution of a manifold-valued process ξ_t is described by first defining an \mathbb{R}^d -valued stochastic process X_t called the stochastic anti-development of ξ_t . The process ξ_t is subsequently obtained by, first identifying \mathbb{R}^d with the tangent spaces above points on \mathcal{M} and then *developing* ξ_t on the manifold by rolling the tangent spaces along the trajectory of X_t onto \mathcal{M} without slipping. The construction of rolling without slipping relies on the idea of attaching an orthonormal basis at every point of the manifold \mathcal{M} and describing the evolution of this basis. Further details about the rolling without slipping procedure can be found in [36].

Remark 3.6. *The manifold arising from attaching every possible basis to \mathcal{M} is called the orthonormal frame bundle of \mathcal{M} and is denoted by $\mathcal{O}(\mathcal{M})$. The map connecting all the tangent spaces at one point to another is called the connection and is denoted by ∇ . See [36] for more details and [24] for the case where there is time dependence on these objects.*

The process ξ_t is called the stochastic development of X_t . This process can be shown to exist and be uniquely defined even in the case of a time-dependent connection, up to choice of initial conditions (see [24] for details).

The filtering problem on a Cartan-Hadamard flow is concerned with best estimating an (\mathcal{M}, g_t) -valued semi-martingale given observations from the (\mathcal{M}, g_t) -valued semi-martingale η_t , with \mathbb{P} -a.s. continuous sample paths. Such an (\mathcal{M}, g_t) -valued semi-martingale can be described by its stochastic-anti-development, Y_t . Similar to the general Euclidean stochastic filtering problem we assume that Y_t satisfies the following stochastic differential equation

$$\begin{aligned} Z_t &= Z_0 + \int_0^t c(s, \xi_s, Z_s) ds + \int_0^t \alpha(s, Z_s) dB_s, \\ U_t &= U_0 + \sum_{i=1}^d H_i^{\nabla}(U_t) \circ dZ_t - \frac{1}{2} \sum_{\alpha, \beta=1}^d \frac{\partial g}{\partial t}(t, U_t e_{\alpha}, U_t e_{\beta}) V_{\alpha, \beta}(U_t) dt \\ Y_t &\triangleq p(U_t) \end{aligned} \quad (3.5)$$

where \circ is the Stratonovich integral, $(V_{\alpha, \beta})_{\alpha, \beta=1}^d$ are the canonical vector fields the orthogonal vector-fields defined by

$$\begin{aligned} V_{\alpha, \beta} f(u) &\triangleq \frac{\partial f}{\partial s}|_{s=0} (u(I + sE_{\alpha, \beta})), \\ E_{\alpha, \beta} &\triangleq (\delta_{\alpha, \beta} e_i \otimes e_j)_{\alpha, \beta=1}^d, \end{aligned} \quad (3.6)$$

$(H_i^{\nabla})_{i=1}^d$ are the ∇ -horizontal vector fields on \mathcal{M} and $p : \mathcal{O}(\mathcal{M}) \rightarrow \mathcal{M}$ is the projection of defining the orthogonal frame bundle on \mathcal{M} (see [36] for more details on stochastic differential geometry). Following [11, Chapter 22.1] we require that W_t is a standard Brownian motion on \mathbb{R}^d and $\alpha : [0, T] \times C([0, T]; \mathbb{R}^d) \rightarrow \mathbb{R}^{d^2}$ is a non-anticipative nonsingular matrix-valued function. Moreover, we require the flowing uniform Lipschitz condition is satisfied: that there exist some $\kappa, K > 0$, such that for every t, y in the domain of α , if

$$\|\alpha(t, 0)\| + \|\alpha(t, y)^{-1}\| \leq k,$$

then

$$\|\alpha(t, y) - \alpha(t, \tilde{y})\| \leq K(y - \tilde{y})_t^*,$$

and $c : [0, T] \times \mathbb{R}^d \times C([0, T]; \mathbb{R}^d) \rightarrow \mathbb{R}^d$, is a bounded, non-anticipative, Borel measurable in (t, x) and satisfies the uniform Lipschitz condition

$$\|c(t, x, y) - c(t, x, \tilde{y})\| \leq K(y - \tilde{y})_t^*.$$

Denote by \mathcal{F}_t , the augmented right-continuous filtration generated by η_t . If (\mathcal{M}, g_t) is the Euclidean space (\mathbb{R}^D, g_E) , the conditional measure $P(\cdot | \mathcal{F}_t)$ of ξ_t given \mathcal{F}_t exists, and $P(\cdot | \mathcal{F}_t)$ is absolutely continuous with respect to the Lebesgue measure m , then the Radon-Nikodým derivative $\frac{dP(\cdot | \mathcal{F}_t)}{dm}$ exists and the classical filtering problem aims at estimating the conditional density of $\phi(\xi_t)$ by considering

$$\operatorname{argmin}_{z \in L^2(\mathcal{F}_t)} \int_{\mathbb{R}^D} \|\phi(x) - z\|^2 m(dx) = \int_{\mathbb{R}^D} \phi(x) \frac{dP(\cdot | \mathcal{F}_t)}{dm} m(dx)^o,$$

where \cdot^o denotes the optional projection and ϕ is a suitable function (see [11, Chapter 22] for more details). In the case where \mathcal{M} is strictly a sub-manifold of \mathbb{R}^D , and ξ_t and η_t take values in \mathcal{M} , then there are two difficulties

- (i) $\frac{dP(\cdot | \mathcal{F}_t)}{dm}$ does not exist,
- (ii) The extrinsic metric $\|x - y\|$ ignores the intrinsic geometry of (\mathcal{M}, g_t) .

It has been proposed, for example in [51], to overcome these issues by replacing the Euclidean metric with the geodesic distance on (\mathcal{M}, g_t) and to replace the Lebesgue measure with the measure μ induced by the Riemann volume form on (\mathcal{M}, g_t) . We note that it is not clear that this minimizer exists in general. Of course, this essentially reduces the problem to the classical filtering problem when (\mathcal{M}, g_t) is Euclidean space. However, we propose a few extensions of this formulation to better generalize the non-Euclidean filtering problem.

Note that it is possible that in a finite amount of time, ξ_t leaves the manifold \mathcal{M} . In the case where no semi-martingale leaves (\mathcal{M}, g_t) in a finite amount of time we will say that (\mathcal{M}, g_t) is stochastically complete. We make the following assumptions.

Assumption 3.7. Denote by μ_t the measure induced by the Riemannian volume form V_{g_t} at time t . For every $t \in [0, \infty)$ assume that

- (i) ξ_t and η_t take values in the Cartan-Hadamard flow (\mathcal{M}, g_t) ,
- (ii) (\mathcal{M}, g_t) is stochastically complete³,
- (iii) The conditional measure $\mathbb{P}_{X|\mathcal{F}_t}$ of ξ_t given \mathcal{F}_t exists, is concentrated on \mathcal{M} , and is absolutely continuous with respect to μ_t ,
- (iv) There exists a point $y \in \mathcal{M}$ such that

$$\int_{\mathcal{M}} d_{\mathcal{M}}^2(x, y) p_{\phi(X_t)|\mathcal{F}_t}(x) \mu_t(dx) < \infty,$$

where the Radon-Nikodým derivative $\frac{d\mathbb{P}_{X|\mathcal{F}_t}}{d\mu_t}$ is denoted by $p_{\phi(X_t)|\mathcal{F}_t}$,

³ A general sufficient condition for stochastic completeness requires that $\int_0^\infty \frac{r}{\ln(B(r, x_0))} dr = \infty$ for any geodesic ball $B(r, x_0)$ centred at any point $x_0 \in \mathcal{M}$ (see [22] for details).

(v) Both ξ_t and η_t are defined on the same complete probability space $(\Omega, \mathcal{F}, (\mathcal{F}_t)_{[0,\infty]}, \mathbb{P})$, where $(\mathcal{F}_t)_{[0,\infty]}$ is a right-continuous filtration of sub- σ -algebras of \mathcal{F}_t containing all the null-sets of \mathcal{F} ,

(vi) The paths of ξ_t are càdlàg, \mathbb{P} -a.s.

Example 3.8. Suppose $(\mathcal{M}, g_t) = (\mathbb{R}^d, g_E)$, let X and Y be an \mathbb{R}^d -valued random vectors and let $\{e_i\}_{i=1}^d$ be an orthonormal basis of \mathbb{R}^d . The Riemannian barycenter, defined by

$$\operatorname{argmin}_{x \in \mathbb{R}^d} \int_{\mathbb{R}^d} d_E^2(x, z) p_{X|\mathcal{F}_t}(x) \mu(dx)$$

may be related to the conditional expectation in the following way

$$\begin{aligned} \operatorname{argmin}_{x \in \mathbb{R}^d} \int_{\mathbb{R}^d} d_E^2(x, z) p_{X|\mathcal{F}_t}(x) \mu(dx) &= \operatorname{argmin}_{z \in \mathbb{R}^d} \int_{\mathbb{R}^d} \|x - z\|^2 p_{X|\mathcal{F}_t}(x) \mu(dx) \\ &= \operatorname{argmin}_{z \in \mathbb{R}^d} \int_{\mathbb{R}^d} \left\| \sum_{i=1}^d \langle (x - z), e_i \rangle e_i \right\|^2 p_{X|\mathcal{F}_t}(x) \mu(dx) \\ &= \sum_{i=1}^d e_i \left[\operatorname{argmin}_{z \in \mathbb{R}^d} \int_{\mathbb{R}^d} \|\langle (x - z), e_i \rangle\|^2 p_{X|\mathcal{F}_t}(x) \mu(dx) \right] \\ &= \sum_{i=1}^d e_i \mathbb{E} [\langle X, e_i \rangle \mid \mathcal{F}_t]. \end{aligned}$$

In particular if $d \geq 1$ and ϕ is of co-dimension $d - 1$ then above expression reduces to the usual univariate conditional expectation.⁴

Lemma 3.9. Under Assumption 3.7 (iii) and (iv), the minimizer of

$$\int_{\mathbb{R}^d} d_E^2(x, z) p_{X|\mathcal{F}_t}(x) \mu(dx), \quad (3.7)$$

exists globally on (\mathcal{M}, g) .

Proof. Note that $\nu(A) \triangleq \int_{\mathcal{M}} 1_A p_{\phi(X_t)|\mathcal{F}_t}(x) \mu_t(dx)$ defines a measure concentrated on \mathcal{M} such that Assumption 3.7 (iv) holds. Since in addition (\mathcal{M}, g_t) is a Cartan-Hadamard manifold then [1, Exercise 5.11] implies that the minimizer of equation (3.7) exists and is unique. \square

Definition 3.10 (Intrinsic Conditional Expectation). Let (\mathcal{M}, g_t) be a Cartan-Hadamard manifold and let ξ_t be an \mathcal{M} -valued semi-martingale. Let $\phi \in C^2(\mathcal{M}; \mathcal{M})$ such that there is a modification $\tilde{\xi}_t$ of ξ_t such that Assumption 3.7 holds when ξ_t is replaced by $\phi(\tilde{\xi}_t)$. For any such ϕ , the intrinsic conditional expectation of $\phi(\xi_t)$ given \mathcal{F}_t , denoted by $\mathbb{E}_{\mathbb{P}}^{g_t} [\phi(\xi_t) \mid \mathcal{F}_t]$, is defined as

$$\mathbb{E}_{\mathbb{P}}^{g_t} [\phi(\xi_t) \mid \mathcal{F}_t] \triangleq \operatorname{argmin}_{x \in \mathcal{M}} \int_{\mathcal{M}} d_{g_t}^2(x, z) p_{\phi(\xi_t)|\mathcal{F}_t}(x) \mu(dx). \quad (3.8)$$

⁴ If $d = 1$ and the co-dimension of ϕ is 1 then $p_{X|\mathcal{F}_t}$ is again equal to $\mathbb{E}[X \mid \mathcal{F}_t]$.

Our formulation of the filtering problem on a Cartan-Hadamard flow, seeks to find the density, which we denote by $\pi_t^{\mathcal{M}}(\phi)$, of the optional projection $\mathbb{E}_{\mathbb{P}}^{g_t}[\phi(\xi_t) \mid \mathcal{F}_t]^o$ of the stochastic process of equation (3.8). We solve the Cartan-Hadamard flow filtering problem by showing it can be obtained as the limit of the solution to certain classical filtering problems. Therefore, its dynamics can be obtained asymptotically as the limit of certain Euclidean optimal filters given by the Kushner-Stratonovich formula.

Lemma 3.11. *Let $\Delta > 0$ and let ξ_t be a (\mathcal{M}, g_t) -valued semi-martingale. Under Assumption 3.7 (ii)-(v) the following equation holds*

$$\begin{aligned} \int_{\mathcal{M}} d_{g_t}^2(\phi(x), z) p_{X \mid \mathcal{F}_t}(x) \mu_t(dx) &= \int_{\mathbb{R}^d} d_{g_t}^2(\phi(x), z) p_{X \mid \mathcal{F}_t}^{\Delta}(x) m(dx), \\ p_{X \mid \mathcal{F}_t}^{\Delta}(x) &\triangleq p_{X \mid \mathcal{F}_t}(x) J_t^{\Delta}(\omega)(x), \\ J_t^{\Delta}(\omega)(\cdot) &\triangleq |J(\log(\cdot, \phi(\xi_{t_i}^{\mathfrak{r}})))|. \end{aligned} \quad (3.9)$$

Proof. Since $\text{Cut}(x)$ is of μ_t -measure 0 for any point in a Riemannian manifold, the same is true for $\text{Cut}(\xi_{t_i}^{\mathfrak{r}})$ for every $\omega \in \Omega$. Since the conditional measure ν_t of $\xi_t^{\mathfrak{r}}$ given \mathcal{F}_t is absolutely continuous with respect to μ_t for every $t \in [0, \infty)$ then for every $\omega \in \Omega$, $\text{Cut}(\xi_{t_i}^{\mathfrak{r}})$ is of ν_t -measure 0. Therefore we may work directly on $\mathcal{M} - \text{Cut}(\xi_{t_i}^{\mathfrak{r}})$.

On $\mathcal{M} - \text{Cut}(\xi_{t_i}^{\mathfrak{r}})$, $\log(\cdot, \xi_{t_i}^{\mathfrak{r}})$ and its inverse $\text{Exp}(\cdot, \xi_{t_i}^{\mathfrak{r}})$ define a diffeomorphism onto \mathbb{R}^d for every $\omega \in \Omega$. Therefore equation (3.9) reduces to the change of variables formula. \square

Let $\Xi_t(\omega) = \mathcal{M} - \text{Cut}(\phi(\xi_t^{\mathfrak{r}}))$ define the non-anticipative functions $\Lambda_{\Delta}(\cdot)$ and $\Lambda_{\Delta}^{\star}(\cdot)$ on the path of $\xi_t^{\mathfrak{r}}$ are defined as

$$\Lambda_{\Delta}(\xi_t^{\mathfrak{r}})(\omega) \triangleq \begin{cases} \log^{g_t}(\xi_{t-(\Delta \wedge 0)}^{\mathfrak{r}}(\omega), \xi_t^{\mathfrak{r}}(\omega)), & \text{if } \{\xi_t^{\mathfrak{r}}(\omega), \xi_{t-(\Delta \wedge 0)}^{\mathfrak{r}}(\omega)\} \subseteq \Xi_t(\omega) \\ 0, & \text{otherwise} \end{cases}$$

and

$$\Lambda_{\Delta}^{\star}(\phi)(\cdot)(\omega) \triangleq \begin{cases} \log^{g_t}(\phi(\xi_t^{\mathfrak{r}}(\omega)), \cdot) \circ \phi \circ \text{Exp}^{g_t}(\phi(\xi_t^{\mathfrak{r}}(\omega)), \cdot), & \text{if } \{\phi(\xi_t^{\mathfrak{r}}(\omega)), \phi(\xi_{t-(\Delta \wedge 0)}^{\mathfrak{r}}(\omega))\} \subseteq \Xi_t(\omega) \\ 0, & \text{otherwise} \end{cases}$$

for every $\omega \in \Omega$. If $\xi_t^{\mathfrak{r}}$ has \mathbb{P} -a.s right-continuous paths then so must $\phi(\xi_t^{\mathfrak{r}})$, since ϕ is of class $C^{1,2}$. Since $\log(p, q)$ is of class C^{∞} in both p and in q then it follows that for \mathbb{P} -almost every $\omega \in \Omega$

$$\begin{aligned} \lim_{\Delta \rightarrow 0^+} \log(\phi(\xi_{t-(\Delta \wedge 0)}^{\mathfrak{r}}(\omega)), \phi(\xi_t^{\mathfrak{r}}(\omega)))t &= \lim_{\Delta \rightarrow 0^+} \log(\phi(\xi_{t-(\Delta \wedge 0)}^{\mathfrak{r}}(\omega)), \phi(\xi_t^{\mathfrak{r}}(\omega)))t \\ &= \log(\phi(\xi_{t-(\Delta \wedge 0)}^{\mathfrak{r}}(\omega)), \phi(\xi_t^{\mathfrak{r}}(\omega)))t \\ &= \|0\| = 0. \end{aligned} \quad (3.10)$$

Likewise, the \mathbb{P} -a.s. right-continuity of the paths of ξ_t imply that

$$\begin{aligned} \lim_{\Delta \rightarrow 0^+} \log(\phi(\xi_{t-(\Delta \wedge 0)}^{\mathfrak{r}}(\omega)), Z)t &= \lim_{\Delta \rightarrow 0^+} \log(\phi(\xi_{t-(\Delta \wedge 0)}^{\mathfrak{r}}(\omega)), Z)t \\ &= \log(\phi(\xi_t^{\mathfrak{r}}(\omega)), \phi(\xi_t^{\mathfrak{r}}(\omega)))t. \end{aligned} \quad (3.11)$$

Moreover since (\mathcal{M}, g_t) is stochastically complete and is Cartan-Hadamard, then ξ_t^r never leaves \mathcal{M} and the map $\text{Log}^{g_t}(\cdot, \cdot)$ maps are defined globally on \mathcal{M} for every time $t \in [0, \infty)$. Hence equations (3.10) and (3.11) are defined for every $(t, x) \in [0, \infty) \times \mathcal{M}$, \mathbb{P} -a.s. Combining those two equations together with the continuity of $\|\cdot\|^2$, we may conclude that

$$\lim_{\Delta \rightarrow 0^+} \|(\Lambda_\Delta^*(\phi)(\Lambda_\Delta(\xi_t^r)) - Z)\|^2 = d_{g_t}(\phi(\xi_t^r), Z)^2, \quad (3.12)$$

for every $Z \in L^2(\mathcal{F}_t)$, \mathbb{P} -a.s. In particular this implies that

$$\lim_{\Delta \rightarrow 0^+} J_t^\Delta = I.$$

We assume that the geometry of (\mathcal{M}, g_t) is sufficiently well-behaved near the trajectory of ξ_t . More precisely, we make the following integrability and path-regularity assumptions.

Assumption 3.12. *Assume that ϕ is a twice continuously differentiable functions from \mathcal{M} to itself such that*

(i) *Assumption 3.7 holds when replacing \mathcal{F}_t by the σ -algebra generated by any continuous \mathcal{M} -valued semi-martingale ζ_t*

(ii) *There exists some $\delta > 0$, such that for every $0 \leq \Delta < \delta$*

$$0 \leq \|(\Lambda_\Delta^*(\phi)(\Lambda_\Delta(\xi_t^r)) - Z)\| \leq \|(\Lambda_\delta^*(\phi)(\Lambda_\delta(\xi_t^r)) - Z)\|. \quad (3.13)$$

(iii) $\mathbb{E} \left[J_t^\delta \|(\Lambda_\delta^*(\phi)(\Lambda_\delta(\xi_t^r)) - Z)\|^2 \right] < \infty$.

Under Assumption 3.12 (iii), we know that the random variable

$$\|(\Lambda_\delta^*(\phi)(\Lambda_\delta(\xi_t^r)) - Z)\|^2,$$

is integrable. Therefore, Assumption 3.12 (ii) and the monotonicity of integration imply that the Lebesgue dominated convergence theorem may be applied to the \mathbb{P} -a.s. point-wise convergence illustrated in equation (3.12) to conclude that

$$\begin{aligned} \lim_{\Delta \rightarrow 0^+} \mathbb{E} \left[J_t^\Delta \|(\Lambda_\Delta^*(\phi)(\Lambda_\Delta(\xi_t^r)) - Z)\|^2 \right] &= \mathbb{E} \left[\lim_{\Delta \rightarrow 0^+} J_t^\Delta \lim_{\Delta \rightarrow 0^+} \|(\Lambda_\Delta^*(\phi)(\Lambda_\Delta(\xi_t^r)) - Z)\|^2 \right] \\ &= \mathbb{E} \left[\|\text{Log}^{g_t}(Z, \phi(\xi_t^r))\|^2 \right] \\ &= \mathbb{E} \left[d_{g_t}^2(\phi(\xi_t^r), Z) \right] \end{aligned} \quad (3.14)$$

In the last equation, we have used the fact that $\|\text{Log}(p, q)\|^2 = d^2(p, q)$ for every p in the cut-locus of q in a Riemannian manifold (see [37] for details), the fact that any Cartan-Hadamard manifold has empty cut-loci as well as and Lemma 3.11. We may summarize the preceding discussion in the following lemma.

Lemma 3.13. *If ξ_t is a semi-martingale with right-continuous sample paths \mathbb{P} -a.s. and Assumption 3.12 holds then*

$$\lim_{\Delta \rightarrow 0^+} \mathbb{E} \left[\|(\Lambda_\Delta^*(\phi)(\Lambda_\Delta(\xi_t^r)) - Z)\|^2 \right] = \mathbb{E} \left[d_{g_t}^2(\phi(\xi_t^r), Z) \right]. \quad (3.15)$$

We have proved that the triangulated objective function converges to the non-Euclidean objective function. We would also like to be able to compute bounds on the error incurred by triangulating the filtering problem's objective function. To achieve this we appeal to the geometry of non-positive curvature spaces. For every \mathcal{M} -valued random element, we first consider the closure of the random geodesic ball about $\xi_{t-(\Delta \wedge 0)}^r(\omega)$ with the stochastic radius

$$\rho(\omega) \triangleq 2 \max \left\{ d^{g_t}(Z(\omega), \xi_{t-(\Delta \wedge 0)}^r(\omega)), d^{g_t}(\xi_t^r(\omega), \xi_{t-(\Delta \wedge 0)}^r(\omega)) \right\}.$$

We denote this geodesic ball by $\mathbb{B}(\omega)$. For every $t \in [0, \infty)$ and every $\omega \in \Omega$, the pair $(\mathbb{B}(\omega), g_t|_{\mathbb{B}(\omega)})$ defines a connected, complete, compact Riemannian manifold of negative-curvature on its interior. The Nash embedding theorem [47] implies that we may isometrically embed $(\mathbb{B}(\omega), g_t|_{\mathbb{B}(\omega)})$ into \mathbb{R}^D for a suitably large $D \in \mathbb{N}$. We denote this isometric embedding by ϕ . Since $\mathbb{B}(\omega)$ is compact, it is bounded and by the continuity of ϕ , $\phi(\mathbb{B}(\omega))$ must equally be bounded in \mathbb{R}^D . Therefore, the diffeomorphism

$$(x_1, \dots, x_D) \mapsto (x_1 + 1 + \max\{|x_1| : (x_1, \dots, x_D) \in \phi(\mathbb{B}(\omega))\}, \dots, x_D)$$

is well-defined and isometrically takes the compact manifold $\phi(\mathbb{B}(\omega))$ into a compact manifold lying in the upper-half space

$$\{x \in \mathbb{R}^D : x_1 > 0\}.$$

Therefore, there is no loss in generality in may assuming that $(\mathbb{B}(\omega), g_t|_{\mathbb{B}(\omega)})$ is isometrically embedded into the upper half space. Since Euclidean space \mathbb{R}^D is a separable, class C^∞ smooth manifold then the upper-half space must also be a separable, connected, class C^∞ smooth manifold. Therefore, the main result of [57] implies that there exists a Riemannian metric $G^t(\omega)$ on \mathbb{R}^D which when restricted to $\phi(\mathbb{B}(\omega))$ is equal to g^t , moreover all geodesics between any two points $p, q \in \phi(\mathbb{B}(\omega))$ with respect to G^t are geodesics with respect to g^t and so lie entirely within $\phi(\mathbb{B}(\omega))$.

Since any isometric embedding is a conformal mapping (see, for example, [37] for more details) then the sectional curvatures of $\phi(\mathbb{B}(\omega))$ and $\mathbb{B}(\omega)$ are identical, let us denote them by $R(x)$. Since the Riemannian manifold (\mathcal{M}, g_t) is Cartan-Hadamard the sectional curvature on all of \mathcal{M} is bounded above by 0, in particular this must be the case for $\mathbb{B}(\omega)$. Since the map $x \mapsto R(x)$ is continuous and $\mathbb{B}(\omega)$ is compact then it must achieve its infimum. Therefore for every $t \in [0, \infty)$, every $\omega \in \Omega$ and every \mathcal{M} -valued random element Z there exists a non-negative number $K_Z^t(\omega)$ such that

$$R(x) \in [-K_Z^t(\omega), 0]. \quad (3.16)$$

Recall that $(\mathbb{B}(\omega), g_t|_{\mathbb{B}(\omega)})$ was embedded into the upper-half space. Alongside $g_t|_{\mathbb{B}(\omega)}$, we consider two additional Riemannian metrics on the upper-half space. The first is the restriction of the Euclidean metric g_E to the upper-half space. For the second, we use the fact that for every $k < 0$, there exists a unique Riemannian metric on the upper-half space with constant negative curvature k , called the hyperbolic metric on the upper-half space model of hyperbolic space. In particular, setting $k = -K_Z^t(\omega)$ we denote the hyperbolic metric with constant sectional curvature $-K_Z^t(\omega)$ by $g_{Z,\omega}^t$.

In particular since the sectional curvature $R(x)$ of $g_t|_{\mathbb{B}(\omega)}$ is bounded between the sectional curvatures of $g_{Z,\omega}^t$ and g_E , respectively when restricted to $\phi(\mathbb{B}(\omega))$. Hence [1, Proposition 5.3]

implies that for any points $A, B, C \in \mathbb{B}(\omega)$

$$\angle(\gamma_{[A,B]}^K(0), \gamma_{[B,C]}^K(0)) \leq \angle(\gamma_{[A,B]}^t(0), \gamma_{[B,C]}^t(0)) \leq \angle(\gamma_{[A,B]}^E(0), \gamma_{[B,C]}^E(0)) \quad (3.17)$$

where γ^K , γ^t and γ^E are the geodesics for the Riemannian metrics $g_{Z,\omega}^t, g_t, g^E$ connecting their respective points on the upper-half space⁵. Define the angles α, β , and γ relative to the points

Comparison of Triangles

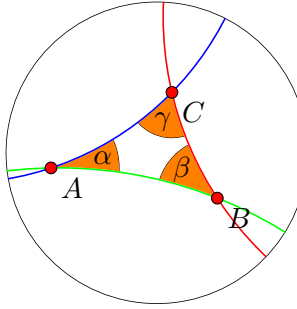


Figure 2: An illustration of the fact that the angles on Riemannian manifold with negative curvature are each strictly smaller than the corresponding Euclidean triangle's angles.

A, B , and C as in figure 2. Moreover, denoting by a, b, c respectively, the lengths of the geodesic curves opposite to the angles α, β and γ respectively. The generalized cosine inequalities of [1, Proposition 5.2] imply that

$$c \in \left[\sqrt{a^2 + b^2 - 2ab \cos(\gamma)}, b \cos(\alpha) + a \cos(\beta) \right]. \quad (3.18)$$

Combining equations (3.17) and (3.18) using the monotonicity of $\cos(\cdot)$ on $[0, \pi]$, it follows that $\|\text{Log}^{g_t}(B, A) - \text{Log}^{g_E}(B, A)\|$ is contained within $[L, R]$ where

$$\begin{aligned} L^2 &\triangleq \left(\|\text{Log}^{g_t}(B, C)^2\|^2 + \|\text{Log}^{g_t}(A, C)^2\|^2 - 2\|\text{Log}^{g_t}(B, C)^2\| \|\text{Log}^{g_t}(B, A)^2\| \cos(\alpha^E) \right) \\ &\quad - \left(\|\text{Log}^{g_t}(B, C)^2\|^2 + \|\text{Log}^{g_t}(A, C)^2\|^2 - 2\|\text{Log}^{g_t}(B, C)^2\| \|\text{Log}^{g_t}(B, A)^2\| \cos(\alpha^K) \right) \\ &= 2\|\text{Log}^{g_t}(B, C)^2\| \|\text{Log}^{g_t}(B, A)\|^2 (\cos(\alpha^E) - \cos(\alpha^K)) \\ R &\triangleq \left(\|\text{Log}^{g_t}(A, C)^2\| \cos(\alpha^E) + \|\text{Log}^{g_t}(B, C)^2\| \cos(\beta^E) \right) \\ &\quad - \left(\|\text{Log}^{g_t}(A, C)^2\| \cos(\alpha^K) + \|\text{Log}^{g_t}(B, C)^2\| \cos(\beta^K) \right) \\ &= \|\text{Log}^{g_t}(A, C)^2\| (\cos(\alpha^E) - \cos(\alpha^K)) + \|\text{Log}^{g_t}(B, C)^2\| (\cos(\beta^E) - \cos(\beta^K)). \end{aligned} \quad (3.19)$$

In particular, setting A, B , and C to be $\xi_{t-(\Delta \wedge 0)}^{\mathbf{r}}(\omega), \xi_t^{\mathbf{r}}(\omega)$ and $Z(\omega)$, respectively, we may draw the following conclusion.

Theorem 3.14. *Let ξ_t be an (\mathcal{M}, g_t) -valued semi-martingale, and let ϕ be such that Assumptions 3.7 and 3.12 are satisfied. Then, for \mathbb{P} -a.e. $\omega \in \Omega$ and for every $Z \in L^2(\mathcal{F}_t)$ define the*

⁵ Note that though the points A, B, C lie on the manifold $\phi(\mathbb{B}(\omega))$, the geodesics obtained from the Euclidean and hyperbolic metrics may leave the manifold, but will always be contained in the upper-half space itself. On the other-hand the geodesics of G^t are contained within the embedded manifold, as is desired.

non-anticipative functional Err on the path of ξ_t^r measuring the triangulation error by

$$\text{Err}(\xi_t^r, \Delta, Z, \phi) \triangleq \left| \mathbb{E} \left[d_t^2 \left(\xi_{t-(\Delta \wedge 0)}^r(\omega), Z \right) \right] - \mathbb{E} \left[J_t^\Delta \left\| (\Lambda_\Delta^\star(\phi)(\Lambda_\Delta(\xi_t^r)) - \Lambda_\Delta Z) \right\|^2 \right] \right|. \quad (3.20)$$

Then

$$\lim_{\Delta \rightarrow 0^+} \text{Err}(\xi_t^r, \Delta, Z, \phi) = 0. \quad (3.21)$$

Moreover, for every $\Delta \in [0, \delta)$, and every $Z \in L^2(\mathcal{F}_t)$, we have the following bounds on the linearization error $\text{Err}(\xi_t^r, \Delta, Z, \phi)$

$$\begin{aligned} \text{Err} &\in [L, R] \\ L &\triangleq \mathbb{E} \left[\sqrt{2\|\Lambda_\Delta(Z)\|^2\|\Lambda_\Delta(\xi_t^r)\|^2(\cos(\alpha_t^E) - \cos(\alpha_t^K))} \right] \\ R &\triangleq \mathbb{E} \left[\|\Lambda_\Delta(Z)\|^2(\cos(\alpha_t^E) - \cos(\alpha_t^K)) + \|\Lambda_\Delta(\xi_t^r)\|^2(\cos(\beta_t^E) - \cos(\beta_t^K)) \right] \\ \alpha_t^E(\omega) &\triangleq \angle \left(\gamma_{[\xi_{t-(\Delta \wedge 0)}^r(\omega), \xi_t^r(\omega)], Z(\omega)]}^E, \gamma_{[\xi_{t-(\Delta \wedge 0)}^r(\omega), Z(\omega)]}^E \right) \\ \alpha_t^K(\omega) &\triangleq \angle \left(\gamma_{[\xi_{t-(\Delta \wedge 0)}^r(\omega), \xi_t^r(\omega)], Z(\omega)]}^K, \gamma_{[\xi_{t-(\Delta \wedge 0)}^r(\omega), Z(\omega)]}^K \right) \\ \beta_t^E(\omega) &\triangleq \angle \left(\gamma_{[Z(\omega), \xi_t^r(\omega)], Z(\omega)]}^E, \gamma_{[Z(\omega), \xi_{t-(\Delta \wedge 0)}^r(\omega)], Z(\omega)]}^E \right) \\ \beta_t^K(\omega) &\triangleq \angle \left(\gamma_{[Z(\omega), \xi_t^r(\omega)], Z(\omega)]}^K, \gamma_{[Z(\omega), \xi_{t-(\Delta \wedge 0)}^r(\omega)], Z(\omega)]}^K \right). \end{aligned} \quad (3.22)$$

Proof. The proof of equation (3.21) follows from equation (3.15) after applying the change of measure from Lemma 3.11. Equation (3.22) was proved in the discussion preceding the theorem. \square

Theorem 3.14 shows that asymptotically in Δ , the error induced by linearizing the Riemannian distance d_{gt} is zero. Moreover, it can be explicitly estimated if the maximum local sectional curvature is computed. Over a suitably general class of semi-martingales, which are stable under minimization efforts, we may extend Theorem 3.14 to asymptotically estimate the dynamics of the non-Euclidean filter $\pi_t^{\mathcal{M}}(\phi)$ by a sequence of linear filters. We briefly take the time to review some relevant theory of Γ -convergence of [7] and use it to motivate the introduction of a class of semi-martingales conducive to the solution of our problem.

Formally, a sequence F_n of functionals on a metric space (X, d) is said to Γ -converge to a functional F on (X, d) if and only if the following two limits exist and are equal

$$\begin{aligned} \Gamma\text{-}\overline{\lim}_{n \rightarrow \infty^+} &= \inf \left\{ \overline{\lim}_{n \rightarrow \infty^+} F_n(x_n) : x_n \mapsto x \right\} \\ \Gamma\text{-}\underline{\lim}_{n \rightarrow \infty^+} &= \inf \left\{ \underline{\lim}_{n \rightarrow \infty^+} F_n(x_n) : x_n \mapsto x \right\}. \end{aligned} \quad (3.23)$$

In that case their common value is called the Γ -limit of F_n and is denoted by $\Gamma\text{-}\lim_{n \rightarrow \infty} F_n$. If the functionals grow quickly at extreme points on (X, d) across all $n \in \mathbb{N}$, then the Fundamental Theorem of Γ -convergence (see [7, Theorem 2.10]) implies that any sequence of minimizers of

the F_n converges a minimizer of their Γ -limit. In the case where (X, d) is (\mathbb{R}^d, d_E) and F_n is constant in n , this is equivalent to requiring that the F_n satisfy

$$\frac{\langle F_n(x), x \rangle}{\|x\|} \xrightarrow[\infty]{\|x\|} \infty^+. \quad (3.24)$$

The condition of equation (3.24) is called *coerciveness* and is well studied in the classical optimization literature. The equicoerciveness required in the fundamental theorem of Gamma convergence is an abstraction of equation (3.24). We shall use this property to relate the objective function of the Cartan-Hadamard flow filtering problem and the Euclidean filtering problem's objective function.

Definition 3.15 (Γ -Martingale). *Let \mathcal{M} be a sub-manifold of \mathbb{R}^D and let ξ_t be an \mathbb{R}^D -valued semi-martingale which admits a modification ξ_t^r which satisfies Assumptions 3.7 and 3.12.*

*Let $\delta > \tilde{\delta} > 0$ be as in Assumption 3.12 (ii). Define the set $\Gamma^{1,2}(\xi_t)$ to be the subset of $C^{1,2}([0, \infty) \times \mathcal{M}; \mathcal{M})$ comprised of functions ϕ for which the net, from the space of càdlàg and adapted processes endowed with the weak * -topology, defined by*

$$\left\{ F_\Delta(Z) \triangleq \mathbb{E} \left[J_t^\Delta \left\| \Lambda_\Delta^* (\phi) (\Lambda_\Delta (\xi_t^r)) - \Lambda_\Delta Z \right\| \right] \right\}_{\Delta \in [0, \tilde{\delta})}^o,$$

describes a set of equicoercive functionals whose Γ -limit exists and equals to

$$\int_{\mathcal{M}} d_{g_t}^2(x, z) p_{\phi(\xi_t^r)}(x) \mu(dx).$$

If the map $(t, x) \mapsto x$ is in $\Gamma^{1,2}(\xi_t)$, we say that ξ_t is a Γ -martingale.

The notation $\Gamma^{1,2}(\xi_t)$ is critical for controlling the optimization problem defining the intrinsic conditional expectation. Namely, it sets up the theory of Γ -convergence introduced in [12]. We now provide a general set of conditions under which we can ensure that $\{\pi_t^\Delta(\phi)\}_{0 \leq \Delta < \delta}$ defines a class of Γ -martingales.

Assumption 3.16. *Let \mathcal{M} be a sub-manifold of \mathbb{R}^D and let ξ_t be an \mathbb{R}^D -valued semi-martingale which admits a modification ξ_t^r whose paths are right-continuous and are in \mathcal{M} \mathbb{P} -a.s. Define the set $\Gamma^{1,2}(\xi_t)$ be the subset of $C^{1,2}([0, \infty) \times \mathcal{M}; \mathcal{M})$ comprised of functions ϕ for which*

(i) *There exist $\hat{\delta} > 0$ such that for every $t \in [0, \infty)$ and every $\Delta \in [0, \hat{\delta})$ there exists a $\varepsilon_\Delta > 0$*

$$\pi_t^\Delta(\phi) \triangleq \Lambda_\Delta^{-1} \left(\mathbb{E} \left[J_t^\Delta \Lambda_\Delta^* (\phi) (\Lambda_\Delta (\xi_t^r)) \mid \mathcal{F}_t \right] \right)^o \in B^*, \quad (3.25)$$

for every ϕ satisfying Assumption 3.12, where

$$B^* \triangleq \left\{ x \in f \in \overline{\text{Ball}^*}(\varepsilon_\Delta, \pi_t^{\mathcal{M}}(\phi)) \text{ and } \mathbb{P} \left(\overline{\text{supp}(x)} \subseteq \overline{\mathcal{M}} \right) = 1 \right\},$$

where $\overline{\text{Ball}^}(\varepsilon_\Delta, \pi_t^{\mathcal{M}}(\phi))$ denotes the closure of the ball of radius ε about $\pi_t^{\mathcal{M}}(\phi)$ in the weak * topology.*

(ii) *There exists a $\tilde{\delta} > 0$ such that for every $0 < \Delta_1 \leq \Delta_2 < \tilde{\delta}$ for every $Z \in B^*$*

$$\mathbb{E} \left[J_t^{\Delta_1} \left\| \Lambda_{\Delta_1}^* (\phi) (\Lambda_{\Delta_1} (\xi_t^r)) - \Lambda_{\Delta_1} Z \right\| \right] \leq \mathbb{E} \left[J_t^{\Delta_2} \left\| \Lambda_{\Delta_2}^* (\phi) (\Lambda_{\Delta_2} (\xi_t^r)) - \Lambda_{\Delta_2} Z \right\| \right], \quad (3.26)$$

(iii) Assumption 3.7 holds for $\phi(\xi_t^r)$.

Theorem 3.17. Let ξ_t and $\phi \in \Gamma^{1,2}(\xi_t)$ be such that Assumption 3.16 holds, and let $\{\Delta_n\}_{n \in \mathbb{N}}$ be a monotonically decreasing sequence converging to 0. Then

$$\left(\lim_{n \rightarrow \infty} \pi_t^{\Delta_n}(\phi) \right) = \pi_t^{\mathcal{M}}(\phi), \quad (3.27)$$

where the limit is taken in the weak^{*}-topology. Hence ξ_t is a Γ -martingale.

The following result shows that Γ -martingales are good candidates for a uniform approximation of the non-Euclidean filtering problem.

Corollary 3.18 (Asymptotic Filtering equations for Locally-Triangulated Γ -Martingales). Denote the σ -field generated by ξ_t , by \mathcal{G}_t . Let ξ_t be a Γ -martingale such that for every $\Delta \in (0, \delta)$ there exists a \mathcal{G}_t -martingale N_t^Δ and a process β_t^Δ such that

$$\begin{aligned} \Lambda_\Delta(\xi)_t &= \Lambda_\Delta(\xi)_0 + \int_0^t \beta_s^\Delta ds + N_t^\Delta, \\ \mathbb{E} \left[\int_0^t \beta_s^\Delta ds \right] &< \infty, \\ \mathbb{E} \left[\int_0^t N_s^\Delta ds \right] &< \infty, \end{aligned}$$

and $\phi \in \Gamma^{1,2}(\xi_t)$. Then

(i) For every $\Delta \in (0, \delta)$, let $\{e_i\}_{i=1}^d$ be an orthonormal basis for \mathbb{R}^d and define the set of functions $\{f_i(x)\}_{i=1}^d$ by

$$f_i(t, x) \triangleq \langle \Lambda_\Delta(t, x), e_i \rangle.$$

Then the process \tilde{Y}_t^Δ defined by

$$\begin{aligned} \tilde{Y}_t^\Delta &\triangleq \sum_{i=1}^d f_i(0, \eta_0) e_i + \left\{ \sum_{i=1}^d \int_0^t \frac{\partial f_i}{\partial s}(s, \eta_s) e_i ds + \sum_{i,\alpha=1}^d \int_0^t (U_t e_\alpha) f_i(t, \eta_t) \langle c(s, \xi_s, Z_s), e_\alpha \rangle e_i dt \right. \\ &\quad \left. + \frac{1}{2} \sum_{i,\alpha,\beta,\gamma=1}^d \int_0^t \left[\frac{\partial^2 f_i}{\partial x_\alpha \partial x_\beta}(s, \eta_s) - \Gamma_{\alpha,\beta}^\gamma(t) \frac{\partial f_i}{\partial \gamma} \right] (U_t e_\alpha, U_t e_\beta) (\alpha(t, \eta_t)^\star \alpha(t, \eta_t))_{\alpha,\beta} e_i dt \right\} \\ &\quad + \sum_{i,\alpha=1}^d \int_0^t (U_t e_\alpha) f_i(t, \eta_t) \langle c(s, \xi_s, Z_s), e_\alpha \rangle e_i dW_t^\alpha \end{aligned} \quad (3.28)$$

is a weak solution to the stochastic differential equation

$$S_0 + \int_0^t S_s ds = \Lambda_\Delta(t, \eta_0) + \int_0^t \Lambda_\Delta(t, \eta_s) ds,$$

whose strong solution defines $\Lambda_\Delta(\eta)$.

(ii) For every $\Delta \in (0, \delta)$ write the dynamics of the process $\Lambda_\Delta(\eta_t)$ as

$$\begin{aligned}\Lambda_\Delta(\eta_t) &= \int_0^t c^\Delta(s, X, Y) ds + \int_0^t \alpha^\Delta(s, Y) dW_s \\ \langle N, W^i \rangle_t &= \int_0^t (\lambda_s^\Delta)^i ds,\end{aligned}$$

for some \mathbb{R}^d -valued \mathcal{G}_t -predictable process λ_t^Δ . Then

$$\begin{aligned}\pi_t^\Delta(\phi) &= \pi_0^\Delta(\phi) + \int_0^t (\beta_s^\Delta)^o ds \\ &\quad + \int_0^t \left((\lambda_s^\Delta) + (\alpha_s^\Delta)^{-1}(s, Y) \right) \left(R_s^\Delta - \pi_s^\Delta(\phi) (c^\Delta)^o(\omega, s, Y) \right)^* dV_s^\Delta,\end{aligned}\tag{3.29}$$

R_t^Δ is the optional projection of the process $\pi_t^\Delta(1)c(t, X, Y)$ onto the σ -field \mathcal{F}_t , and where V_s^Δ is the innovations process defined by

$$\begin{aligned}V_t^\Delta &\triangleq \tilde{Y}_t^\Delta - \int_0^t (\alpha^\Delta)^{-1}(s, \Lambda_\Delta(\eta_t)) (c^\Delta)^o(\omega, s, \Lambda_\Delta(\eta_t)) ds \\ \tilde{Y}_t^\Delta &\triangleq \Lambda_\Delta(\eta_0) + \int_0^t \alpha^\Delta(s, \Lambda_\Delta(\eta_s)) d\tilde{Y}^\Delta s.\end{aligned}$$

Definition 3.19 (Locally Triangulated Filter). Let ξ_t be a Γ -Martingale and any let $\phi \in \Gamma^{1,2}(\xi_t)$. We call the process $\pi_t^\Delta(\phi)$, introduced in equation (3.25), the Δ -linearized filter of $\pi_t^\mathcal{M}(\phi)$.

The results presented are computable since they have been reduced to a limit of Euclidean filtering problems which have many known implementation methods. We next show how to use a particle filter to implement these results.

3.2 Implementation of Locally Triangulated Filter

We may implement the locally triangulated filter $\pi_t^\Delta(\phi)$ by modifying particle filtering algorithms. For example consider the following modification of the Auxiliary Sampling/Re-Sampling Particle Filter (ASRS-PF) [50, Algorithm 9.6.1] using ideas of [49].

Definition 3.20 (Locally-Triangulated Auxiliary Sampling/Re-sampling Particle Filter). The local triangulation of the (ASRS-PF) algorithm on the Cartan-Hadamard flow (\mathcal{M}, g_t) is defined by Algorithm 3.2. In Algorithm 3.2, $g_{1,i}$ is a positive function and $g_{2,i+1}$ be a function with the same support as $p_{Z_{i+1}|Z}$.

Algorithm 3.2 corrects the theoretical deficiencies present in [55, Algorithm 17.2] and [52] as well as allowing it to handle general processes. Moreover, time-dependence of the Riemannian geometry is also incorporated. In Algorithm 3.2, Step 2.(i) can be interpreted as an intrinsic likelihood maximization step where the best intrinsic guess of ξ_t is used to triangulate about the

Algorithm 3.2: Locally-Triangulated Auxiliary Sampling/Re-sampling Particle Filter

Data: The \mathcal{M} -valued data $\{y_{t_i}\}_{i=1}^k$, initial distribution η_0 for ξ_t , an initial guess $\bar{\xi}_0$ at ξ_0 , and positive integers N, M , and K ,

Result: The measure $\pi_t^{\Delta, \epsilon}$

1. Generate particles $\{z_0^{(k)}\}_{k=1}^N$ from the initial distribution η_0 . Call this population of particles

$$\mathcal{P}_i \left\{ z_i^{(k)} : k \in \{1, \dots, N\} \right\}$$

obtained at step i from probability distribution π_i^N ; where $\pi_0^N \triangleq 0$.

2. **for** $i \in \{1, \dots, M\}$ **do**

- (i) Geometric Particle Initialization

- (i) Define the Jacobian matrix $J_i \triangleq J \left(\text{Log}(\cdot, \hat{\xi}_{i-1}) \right)$
- (ii) Generate K particles $\{\tilde{u}_i\}_{i=1}^K$ on \mathcal{M} from the distribution $J_i \text{Log}^{g_{t_i}} \left(\hat{\xi}_{i-1}, \eta_{i-1} \right)$,
- (iii) Define the set of particles $\{u_i \triangleq \text{Exp}^{g_{t_i}} \left(\hat{\xi}_{i-1}, \tilde{u}_i \right)\}_{i=1}^K$
- (iv) Compute the empirical intrinsic mean $\bar{y}_i \triangleq \underset{y \in \mathcal{M}}{\text{argmin}} \left(\sum_{i=1}^N \|\text{Log}^{g_t} (y, u_i)\|^2 \right)$
- (v) Define the linearized observation $Y_{t_i} \triangleq \text{Log}^{g_{t_M}} (\bar{y}_i, y_{t_i})$,

- (ii) (ASR) Particle Filtering

- (i) For $k \in \{1, \dots, N\}$, compute

$$\begin{aligned} \tilde{v}_{i+1}^{(k)} &\triangleq g_{1,i+1}(k, z_i^{(k)}) \pi_i^{N,(k)} \\ \tilde{\pi}_{i+1}^{(k)} &\triangleq \frac{\tilde{v}_{i+1}^{(k)}}{\sum_{j=1}^N \tilde{v}_{i+1}^{(j)}} \end{aligned} \quad (3.30)$$

- (ii) Choose N values $\tilde{z}_{i+1}^{(k)}$, $k \in \{1, \dots, N\}$, from \mathcal{P}_i with the probability of choosing $z_i^{(k)}$ being $\tilde{\pi}_i^N$.

- (iii) Generate $\{z_{i+1}^{(k)} \stackrel{D}{\sim} g_{2,i+1} \left(\cdot \mid \tilde{z}_{i+1}^{(k)} \right)\}_{k=1}^N$,

- (iv) Define

$$\begin{aligned} v_{i+1}^{(k)} &\triangleq \frac{p_{Y_{i+1}|Z_{i+1}} \left(y_{i+1} \mid z_{i+1}^{(k)} \right) p_{Z_{i+1}|Z_i} \left(z_{i+1}^{(k)} \mid \tilde{z}_{i+1}^{(k)} \right)}{g_{1,i+1} \left(k, \tilde{z}_{i+1}^{(k)} \right) g_{2,i+1} \left(z_{i+1}^{(k)}, \tilde{z}_{i+1}^{(k)} \right)} \\ \pi_{i+1}^{N,(k)} &\triangleq \frac{v_{i+1}^{(k)}}{\sum_{j=1}^N v_{i+1}^{(j)}}. \end{aligned} \quad (3.31)$$

- (iii) The empirical distribution η_{i+1} of the particles $\{z_{i+1}^{(k)}\}_{k=1}^N$, is then defined by

$$\eta_{i+1}(\phi) \triangleq \left(\sum_{k=1}^N \text{Log}^{g_t} \left(\bar{y}_{i-1}, \phi \left[\text{Exp}^{g_t} \left(\bar{y}_{i-1}, z_{i+1}^{(k)} \right) \right] \right) \cdot \pi_{i+1}^{N,(k)} \right),$$

for any twice-continuously differentiable function ϕ .

current observation. The Locally-Triangulated (ASRS) Particle Filtering algorithm can be used to approximate to arbitrary precision the optimal stochastic filters for the prediction of optimal Markowitz portfolios and estimation of stochastic volatility models as described in Examples 3.4 and 3.5 respectively.

In this section we considered the triangulation of a non-Euclidean particle filtering algorithm. In the next section we consider the case where the triangulation method is applied to a statistical or machine learning algorithm to improve its performance.

4 Geometric Improvement of Algorithms

In this section we consider a method for incorporating additional geometric information into a class of algorithms called learning algorithms. These algorithms may be represented probabilistically as optimization problems. Examples include principal component analysis (PCA), the sparse PCA of [64], the elastic-net of [63], group LASSO regularization of [59], K-means clustering, and penalized maximum likelihood estimation, are all common examples of learning algorithms. We now provide a formal definition which encompass all these cases.

Definition 4.1 (Learning Algorithm). *Let A be an algorithm with input, vectors in \mathbb{R}^d and output n_N vectors in \mathbb{R}^{k_N} . Then A is said to be a learning algorithm if for every $N \in \mathbb{N}$ there exists non-negative functional \mathcal{L}_A^N such that*

$$\begin{aligned} \mathcal{L}_A^N : & \mathbb{R}^{n_N \times k_N} \times \mathbb{R}^{N \times d} \rightarrow \mathbb{R} \\ A(x_1, \dots, x_N) = & \underset{\beta \in \mathbb{R}^{n_N \times k_N}}{\operatorname{arginf}} \mathcal{L}_A^N(\beta \mid \otimes_{i=1}^N x_i e_i), \end{aligned} \quad (4.1)$$

holds \mathbb{P} -a.s. The triple $\left(\{\mathcal{L}_A^N\}_{N \in \mathbb{N}}, \{n_N\}_{N \in \mathbb{N}}, \{k_N\}_{N \in \mathbb{N}}\right)$ is said to be a probabilistic representation for the learning algorithm A . The quantity

$$\varepsilon \triangleq \inf_{\beta \in \mathbb{R}^{n_N \times k_N}} \mathcal{L}_A^N(\beta \mid \otimes_{i=1}^N x_i e_i),$$

is termed the learning error of A .

These algorithms are extended to simultaneously optimize a Euclidean objective function with a non-Euclidean penalty which incorporates additional information.

Definition 4.2 (Geometric Improvement). *Let A be a learning algorithm with probabilistic representation $\left(\{\mathcal{L}_A^N\}_{N \in \mathbb{N}}, \{n_N\}_{N \in \mathbb{N}}, \{k_N\}_{N \in \mathbb{N}}\right)$, let \mathcal{M} be a d -dimensional sub-manifold of \mathbb{R}^D , let ξ_t be an \mathbb{R}^D -valued stochastic process which admits a modification \tilde{X}_t taking values in \mathcal{M} . For every set of set N ordered, bounded stopping times $\tau \triangleq \{\tau_i\}_{i=1}^N$, every flow (\mathcal{M}, g_t) on \mathcal{M} and every set $I = \{i\}_{i=1}^K$ of K order d multi-indices; define the improvement of A by $((\mathcal{M}, g_t), \tau)$ is defined by Algorithm 4.1.*

Algorithm 4.1: Geometric Improvement

Data: The \mathcal{M} -valued data $\left\{\tilde{X}_{\tau_i}\right\}_{i=1}^N$,

Result: An element $\beta \in \mathbb{R}^{n_N \times k_N}$

(i) Generate a grid $\{\tilde{x}_i\}_{i \in I}$ in \mathbb{R}^d ,

(ii) Generate the set of points $\{\text{Log}^{g_0}(\tilde{x}_i, x_\Delta)\}_{i \in I}$ on \mathcal{M} ,

(iii) Define a finite ordered partition $\{\lambda_s\}_{s=1}^S$ of $[0, 1]$, where $\lambda_0 = 0$ and $\lambda_S = 1$,

(iv) **for** $s \in \{1, \dots, S\}$ **do**

(i) **for** $i \in I$ **do**

Compute $(\beta_i^{\lambda_s}, \epsilon_i^{\lambda_s})$ defined by

$$\left. \begin{aligned} \beta_i^{\lambda_s} &\triangleq \underset{\beta \in \mathbb{R}^{n_N \times k_N}}{\operatorname{arginf}} \lambda_s \mathcal{L}_A^N \left(\beta \mid \otimes_{j=1}^N \tilde{X}_{\tau_j} e_j \right) + (1 - \lambda_s) \mathcal{L}_A^N \left(\beta \mid \otimes_{j=1}^N \text{Log}^{g_{\tau_i}} \left(\tilde{X}_{\tau_j}, x_i \right) e_j \right) \\ \epsilon_i^{\lambda} &\triangleq \inf_{\beta \in \mathbb{R}^{n_N \times k_N}} \lambda \mathcal{L}_A^N \left(\beta \mid \otimes_{j=1}^N \tilde{X}_{\tau_j} e_j \right) + (1 - \lambda) \mathcal{L}_A^N \left(\beta \mid \otimes_{j=1}^N \text{Log}^{g_{\tau_i}} \left(\tilde{X}_{\tau_j}, x_i \right) e_j \right) \end{aligned} \right\} \quad (4.2)$$

(v) Define the function g on $I \times \{1, \dots, s\}$ by $g(i, s) \triangleq \epsilon_i^{\lambda_s}$,

(vi) Set $(\hat{i}, \hat{s}) \triangleq \underset{(i, s) \in I \times \{1, \dots, s\}}{\operatorname{argmin}} g(i, s)$,

(vii) Define $\beta \triangleq \beta_{\hat{i}}^{\lambda_{\hat{s}}}$,

(viii) Define $\epsilon \triangleq \epsilon_{\hat{i}}^{\lambda_{\hat{s}}}$.

Return (β, ϵ) .

The improvement of A is denoted by $\mathbf{A}_{(\mathcal{M}, g_t)}^{x_\Delta | I}$, and the quantity ϵ is called the learning error of $\mathbf{A}_{(\mathcal{M}, g_t)}^{x_\Delta | I}$.

Remark 4.3. When (\mathcal{M}, g_t) is the Euclidean space then A and $\mathbf{A}_{(\mathcal{M}, g_t)}^{x_\Delta | I}$ coincide. If we set $\lambda = 1$ in Definition 4.2, then again A and $\mathbf{A}_{(\mathcal{M}, g_t)}^{x_\Delta | I}$ would coincide. If A is a learning algorithm, $g_t = g_0$ for every t , and we set $\lambda = 0$ in Definition 4.2, then applying $\text{Exp}^{g_0}(\cdot, x_\Delta)$ to the outputs of $\mathbf{A}_{(\mathcal{M}, g_t)}^{x_\Delta | I}$ would give the same result as $A_{(\mathcal{M}, g_t)}^{x_\Delta}$.

By construction of the geometric improvement algorithm the following improvement holds.

Theorem 4.4. Let A be a learning algorithm, I , ξ_t and (\mathcal{M}, g_t) be as in Definition 4.2. Then the learning error ε_L of A and the learning error ϵ of $\mathbf{A}_{(\mathcal{M}, g_t)}^{x_\Delta | I}$ are related by

$$0 \leq \epsilon \leq \varepsilon_L. \quad (4.3)$$

Proof. By definition, I contains $\lambda_0 = 0$. In the case where $\lambda_s = 0$ the quantities $\beta_i^{\lambda_s}$ and $\epsilon_i^{\lambda_s}$ coincide with β and ε_L , by construction. That is,

$$\epsilon = \epsilon_0^{\lambda_0} \text{ and } \beta = \beta_0^{\lambda_0}. \quad (4.4)$$

Since ε_L is chosen to be a minimizer of the set $\left\{ \varepsilon_i^{\lambda_s} : (i, s) \in I \times \{1, \dots, s\} \right\}$, which contains $\epsilon_0^{\lambda_0}$, then equation (4.4) implies that equation (4.3) must hold. \square

Theorem 4.4 implies that incorporating additional geometric information can only improve the results of the algorithm A . Therefore, careful choice of the geometry (\mathcal{M}, g_t) will strictly improve the algorithm's performance. Evidently, the only possible issue is the added computational complexity.

We now illustrate the improvement of the sparse principal component algorithm for calibrating forward rate curves. In this case, our algorithm will by its construction perform better than the sparse principal component analysis algorithm of [23] or principal geodesic analysis introduced in [19].

4.1 Principal Shapes of the Forward-Rate Curve

Example 4.5 (The 2-Factor Gaussian Model G2++). *A popular choice of forward-rate curve is the 2-Factor Gaussian Model, also known as G2++. The popularity of the G2++ model is due to the fact that it can model the entire forward-rate curve and is well suited to principal component analysis on the forward-rate's volatilities. Specifically, the G2++ model only requires the first two principal components of the volatility of the forward-rates to provide a good fit to the forward-rate data.*

$$\begin{aligned} df(t, T) &\triangleq \left(\sigma_{1,1} e^{-a_1(T-t)} + \sigma_{2,2} e^{-a_2(T-t)} \right) dt \\ &\quad + \left(\sigma_{1,1} e^{-a_1(T-t)} + \sigma_{2,1} e^{-a_2(T-t)} \right) dW_t^1 + \sigma_{2,2} e^{-a_2(T-t)} dW_t^2, \end{aligned}$$

where $a_1, a_2, \sigma_{1,1}, \sigma_{2,1}, \sigma_{2,2}$ are non-negative numbers and W_t is a 2-dimensional Brownian motion.

A common way to calibrate HJM models is via principal component analysis on the covariance matrix. In order to proceed with this calibration technique, we must make the assumption that the volatility processes of the HJM model of equation admits a modification of the form

$$a_i(T-t) = \lambda_i g_i(T-t), \quad (4.5)$$

where g_i are differentiable functions. Under this assumption, it can be shown that the HJM model is Gaussian therefore its increments, which are stationary must be normal [30]. The empirical covariance matrix Q is typically constructed by

$$\begin{aligned} Q_{i,j} &\triangleq \text{Cov}(\Delta f(t, T_i), \Delta f(t, T_j)) = \sum_{k=1}^D \sigma_k(T_i - t) \sigma_k(T_j - t) \\ &= \sum_{k=1}^D \lambda_k^2 g_k(T_i - t) g_k(T_j - t). \end{aligned} \quad (4.6)$$

and the first principal components are extracted via

$$\mathbf{w}_{(1)} = \arg \max_{\|\mathbf{w}\|=1} \{\|\mathbf{Q}\mathbf{w}\|^2\} = \arg \max_{\|\mathbf{w}\|\in\mathbb{R}^D} \{\mathbf{w}^* \mathbf{Q}^* \mathbf{Q} \mathbf{w}\} \quad (4.7)$$

as proposed in [30]. Further principal components are then extracted by

$$\begin{aligned} \mathbf{Q}_k &\triangleq \mathbf{Q} - \sum_{s=1}^{k-1} \mathbf{Q} \mathbf{w}_{(s)} \mathbf{w}_{(s)}^* \\ \mathbf{w}_{(k)} &\triangleq \arg \max_{\|\mathbf{w}\|=1} \{\|\mathbf{Q}_k \mathbf{w}\|^2\} = \arg \max_{\mathbf{w} \in \mathbb{R}^D} \left\{ \frac{\mathbf{w}^* \mathbf{Q}_k^* \mathbf{Q}_k \mathbf{w}}{\mathbf{w}^* \mathbf{w}} \right\}, \end{aligned} \quad (4.8)$$

typically the first 3 are used with their interpretation being level, slope and curvature of the forward-rate curve [13]. Once the principal components are obtained typically some form of interpolation is used to bootstrap together the rest of the curve as described in [8].

In order to incorporate the shape information into the PCA calibration of the forward-rate curve we first consider the loop transform of the FRC, then view every data point $\{l(t, \theta)\}_{i=1}^d$ as a point in shape space and use the corresponding improvement of the sparse PCA algorithm to compute the improved sparse principal components of the loop $l(t, T)$. The principal components are then transformed back to improved principal components of the FRC. We summarize an extended version of this procedure in the following algorithm.

Example 4.6 (Improved Sparse PCA Calibration of the FRC). *Assuming that the FRC process $f(t, T)$ can be written as in equation (4.9). The improved sparse principal component calibration of the FRC is the improvement of the sPCA algorithm and is performed as follows. Assume that the loop transform $l(t, \theta)$ of the FRC $f(t, T)$ of admits a modification of the form*

$$a_i(T - t) = \lambda_i g_i(T - t). \quad (4.9)$$

In that case the improved sparse PCA calibration is the reduced dimension FRC \hat{f} constructed from the data according to Algorithm 4.2.

Remark 4.7. *If in Algorithm 4.2 we set $\gamma = 0$ and $\lambda_s = 1$ we recover the objective function of the PCA algorithm of [64, Theorem 1] and, in particular β , are the principal components of the matrix \mathbb{L} . Allowing $\gamma > 0$ but setting $\lambda_s = 0$, we recover the sparse PCA of [64, equation 3.5]. In contrast setting $\lambda_s = 1$ and $\gamma = 0$ we recover principal components of the matrix Λ . These are locally linear approximations of the principal geodesics of [18]. Therefore, the parameter γ controls sparsity of the solution.*

In general, the Algorithm 4.2 can be interpreted as producing principal components which incorporate the shape of the FRC data. We may use these to construct the reduced dimension forward-rate curve \hat{f} using the inverse loop-transform of Lemma 2.8 by

$$\hat{f}(t, T) = \left| \sum_{i=1}^k \beta_i g_i \left(\frac{tT}{2\pi} \right) \right| + \left(\frac{t(f(T) - f(0))}{2\pi} \right). \quad (4.11)$$

Algorithm 4.2: Improved Sparse PCA Calibration of the FRC

Data: The data $\{f(\tau_i, T_j)\}_{i=1, \dots, N; j=1, \dots, D}$,**Result:** A vector $\sigma \in \mathbb{R}^D$ of volatilities for the factors of $f(t, T)$,

- (i) Define the data matrix set $\mathbb{L}_{i,j} \triangleq l_{f(\tau_i)}(\frac{2\pi\theta_j}{T})$ for $i = 1, \dots, N; j = 1, \dots, D$,
- (ii) Construct the singular value decomposition UDV^T of \mathbb{L} ,
- (iii) Construct the principal components $Z = UD$,
- (iv) Generate a grid $\{\tilde{x}_k\}_{k \in I}$ in \mathbb{R}^D ,
- (v) Define a finite ordered partition $\{\lambda_s\}_{s=1}^S$ of $[0, 1]$, where $\lambda_0 = 0$ and $\lambda_S = 1$,
- (vi) **for** $(k, s) \in I \times \{1, \dots, S\}$ **do**
 - (i) Define the data matrix set $\Lambda_{i,j} \triangleq \text{Log}(x_k, \mathbb{L}_{i,j})$ for $i = 1, \dots, N; j = 1, \dots, D$,
 - (ii) Construct the singular value decomposition $v\delta\nu^T$ of Λ ,
 - (iii) Define the matrix $\zeta = v\delta$,
 - (iv) **for** $r \in \{1, \dots, R\}$ **do**
Compute $(\tilde{\beta}_{r,k}^s, \epsilon_{r,k}^s)$ defined by
$$\tilde{\beta}_{r,k}^s \triangleq \underset{\beta \in \mathbb{R}^D}{\text{argmin}} \lambda_s \|Z_r - \mathbb{L}\beta\|_2^2 + \alpha\|\beta\|_1^2 + (1 - \lambda_s) \|\zeta_r - \Lambda \text{Log}(\tilde{x}_k, \beta)\|_2^2 + \gamma\|\beta\|_1$$

$$\epsilon_{r,k}^s \triangleq \underset{\beta \in \mathbb{R}^D}{\text{argmin}} \lambda_s \|Z_r - \mathbb{L}\beta\|_2^2 + \alpha\|\beta\|_1^2 + (1 - \lambda_s) \|\zeta_r - \Lambda \text{Log}(\tilde{x}_k, \beta)\|_2^2 + \gamma\|\beta\|_1$$
- (v) Define $\beta_{r,k}^s \triangleq \frac{\tilde{\beta}_{r,k}^s}{\|\tilde{\beta}_{r,k}^s\|_2}$
- (vii) Define the function g on $I \times \{1, \dots, s\}$ by $g(k, s) \triangleq \sum_{r=1}^R \epsilon_{r,k}^s$,
- (viii) Set $(\hat{k}, \hat{s}) \triangleq \underset{(k,s) \in I \times \{1, \dots, s\}}{\text{argmin}} g(k, s)$,
- (ix) Define $\beta \triangleq \beta_{\hat{i}}^{\lambda_{\hat{s}}}$,
- (x) Define $\epsilon \triangleq \epsilon_{\hat{i}}^{\lambda_{\hat{s}}}$.
Return (β, ϵ) .

5 Summary

In this paper we have reviewed the geometry of stochastic volatility models, introduced the Markowitz manifold, as well as the loop-transform of a forward-rate curve and discussed how the theory of shape may be applied to improve forecasts of bond prices. We have seen that stochastic volatility models and the Markowitz manifold present natural examples of non-positive curvature flows, which we called Cartan-Hadamard flows. Moreover, in this setting we used the local triangulation technique to asymptotically solve a non-Euclidean stochastic filtering problem in a novel way that is both computable and rigorous.

Specifically, Theorem 3.17 shows that the solution to the non-Euclidean optimal filtering problem may be approximated to arbitrary precision, and asymptotically solved in the weak* sense for any Γ -martingale and any $\phi \in \Gamma^{1,2}(\xi_t)$. Moreover, Theorem 3.18 gave explicit weak-dynamics for the triangulated observation process $\Lambda_\Delta(\eta_t)$ as well as explicit dynamics for the locally-triangulated filters $\pi_t^\Delta(\phi)$. Finally, Theorem 3.14 gave explicit bounds for the error locally arising from triangulating the objective function of the non-Euclidean filtering problem; which we have seen must converge to 0 as the geodesic triangles converge to geodesics on (\mathcal{M}, g_t) . Algorithm 3.2 provides a method for numerically solving the non-Euclidean filtering problem using the locally-triangulated auxiliary sampling-resampling particle filter.

In Section 4 we provided a general method, based on the triangulation methods, for incorporating non-Euclidean geometry into any learning algorithm. Theorem 4.4 showed that this improvement procedure can only improve the accuracy of an algorithm. In particular, we showed how to use this result to extend sparse principal component analysis and principal geodesic analysis to incorporate sparsity and geometric information into the PCA algorithm. Using this method we provided an algorithm which is able to make use of geometric information to improve low-dimensional calibrations of the forward-rate curve to bond data.

This paper demonstrates the need to recognize stochastic differential geometry as a powerful modeling and computational tool in finance. The generality of this work allows for subsequent applications in the improvement of many other algorithms in finance. Lastly, we note that our geometric improvement and non-Euclidean filtering results may naturally be applied outside of mathematical finance and can find additional applications in areas which employ filtering and statistical or machine learning methods.

A Proofs

This appendix provides the proofs of Theorem 3.17 and Corollary 3.18.

Proof of Theorem 3.17. Denote by F the objective function

$$F(Z) \triangleq \int_{\mathcal{M}} d_{g_t}^2(\xi_t(\omega), Z(\omega)) p_{X|\mathcal{F}_t}(\omega) \mu(d\omega),$$

of $\pi_t^{\mathcal{M}}(\phi)$. Since B^* is a subset of the closed unit ball in $L^2(\mathcal{F}_t)$, and the Banach-Alaoglu Theorem gives that $\overline{B_\epsilon(\pi_t^{\mathcal{M}}(\phi))}^*$ is weak*-compact, we only need to show that B^* is closed in $\overline{B_\epsilon(\pi_t^{\mathcal{M}}(\phi))}^*$ to conclude that it is weak*-compact. Since $L^2(\mathcal{F}_t)$ is separable we only need to

show that B^* contains all limit points of any sequence within B^* to show it is weak^{*}-closed. Let X_n be a sequence in B^* then for every $n \in \mathbb{N}$

$$\bigcup_{n \in \mathbb{N}} \overline{\text{supp}(X_n)} \subseteq \mathcal{M}.$$

Therefore if $X_n(\omega) \in \mathbb{R}^D - \mathcal{M}$ then for every $\omega \in \Omega$

$$\lim_{n \rightarrow \infty} X_n(\omega) \in \bigcup_{n \in \mathbb{N}} \overline{\text{supp}(X_n)} \subseteq \mathcal{M}.$$

Therefore, $\lim_{n \rightarrow \infty} X_n(\omega) \in \overline{\mathcal{M}}$, hence B^* contains all its limiting points; hence is a sequentially compact subset of a compact separable space, namely $\overline{B_\epsilon(\pi_t^{\mathcal{M}}(\phi))}^*$. Therefore B^* is weak^{*}-compact.

For every $x \in [0, \infty)$, the set $\{Z \in B^* : \mathbb{E} [J_t^\Delta \|\Lambda_\Delta^*(\phi)(\Lambda_\Delta(\xi_t^r)) - Z\|] \geq x\}$ is contained within B^* which itself is compact. Therefore, the sequence $\{\mathbb{E} [J_t^\Delta \|\Lambda_{\Delta_n}^*(\phi)(\Lambda_{\Delta_n}(\xi_t^r)) - \Lambda_{\Delta_n} Z\|]\}_{n \in \mathbb{N}}$ is equicoercive.

Since ξ_t^r has right-continuous paths, and (\mathcal{M}, g) is Cartan-Hadamard, Lemma 3.11 implies that

$$F_n(Z) \triangleq \mathbb{E}_\mu [(\Lambda_{\Delta_n}^*(\phi)(\Lambda_{\Delta_n}(\xi_t^r)) - \Lambda_{\Delta_n} Z)] = \mathbb{E} [J_t^{\Delta_n} \|\Lambda_{\Delta_n}^*(\phi)(\Lambda_{\Delta_n}(\xi_t^r)) - \Lambda_{\Delta_n} Z\|].$$

Since ξ_t is a Γ -martingale and $\phi \in \Gamma^{1,2}(\xi_t)$, Theorem 3.14 implies that $F_n(\cdot)$ converges to the objective function $F(\cdot)$ of $\pi_t^{\mathcal{M}}(\phi)$ on B^* . Assumption 3.7 (ii) implies that the sequence $\{F_n(\cdot)\}_{n \in \mathbb{N}}$ where N is the subset of \mathbb{N} of elements of the form

$$\left\{ n \in \mathbb{N} : \Delta_n < \min \left\{ \delta, \tilde{\delta}, \hat{\delta} \right\} \right\},$$

is monotonically decreasing. Moreover, since B^* is weak^{*}-compact, Dini's Theorem implies that the convergence of $\{F_n(\cdot)\}_{n \in \mathbb{N}}$ must be uniform on B^* to $F(\cdot)$. Since uniform limits of continuous functions are equal to their Γ -limit, then the sequence $\{F_n(\cdot)\}$ must Γ -converge to its uniform limit on B^* . Hence

$$\lim_{n \rightarrow \infty} F_n(\cdot) = F(\cdot),$$

on B^* .

Since $F_n(\cdot)$ is equicoercive and converges in the Γ -sense to $F(\cdot)$ on B^* , then a minimizer of $F_n(\cdot)$ converges to a minimizer of $F(\cdot)$. Lemma 3.11 implied that there exists a unique minimizer of $F(\cdot)$, namely $\pi_t^{\mathcal{M}}(\phi)$ and the unique minimizer of $F_n(\cdot)$ is given by the conditional expectation $\pi_t^{\Delta_n}(\phi)$. Therefore on B^* it follows that

$$\lim_{n \rightarrow \infty} \underset{Z \in B^*}{\text{argmin}} F_n(Z) = \underset{Z \in B^*}{\text{argmin}} F(Z). \quad (\text{A.1})$$

However, Assumption 3.7 (i) implies that optimizing over B^* and over all of $L^2(\mathcal{F}_t)$ are equivalent. Therefore equation (A.1) can be rewritten as

$$\lim_{n \rightarrow \infty} \pi_t^{\Delta_n}(\phi) \triangleq \lim_{n \rightarrow \infty} \underset{Z \in L^2(\mathcal{F}_t)}{\text{argmin}} F_n(Z) = \lim_{n \rightarrow \infty} \underset{Z \in B^*}{\text{argmin}} F_n(Z) = \underset{Z \in B^*}{\text{argmin}} F(Z). \quad (\text{A.2})$$

Lastly, since by definition $\pi_t^{\mathcal{M}}(\phi)$ must have support in $\overline{\mathcal{M}}$ and be in the closed-ball of radius 0 about itself then $\pi_t^{\mathcal{M}}(\phi) \in B^*$. Therefore the right-hand side of equation (A.2) may be rewritten as

$$\lim_{n \rightarrow \infty} \pi_t^{\Delta^n}(\phi) \triangleq \lim_{n \rightarrow \infty} \underset{Z \in L^2(\mathcal{F}_t)}{\operatorname{argmin}} F_n(Z) = \underset{Z \in B^*}{\operatorname{argmin}} F(Z) = \underset{Z \in L^2(\mathcal{F}_t)}{\operatorname{argmin}} F(Z) \triangleq \pi_t^{\mathcal{M}}(\phi). \quad (\text{A.3})$$

Therefore, the result follows. \square

Proof of Corollary 3.18. Since (\mathcal{M}, g_t) is Cartan-Hadamard then every Cut-locus on \mathcal{M} is empty, therefore $\Lambda_{\Delta}(\cdot)$ is of class $C^{\infty}(\mathcal{M}; \mathbb{R}^d)$. Hence the functions $\{f_i(\cdot)\}_{i=1}^d$ are also of class $C^{\infty}(\mathcal{M}; \mathbb{R})$. Therefore

$$\tilde{Y}_t \triangleq \sum_{i=1}^d f_i(t, \eta_t) e_i$$

is a weak solution to the SDE

$$S_t = \Lambda_{\Delta}(t, \eta_0) + \int_0^t \Lambda_{\Delta}(t, \eta_s) dt,$$

(see [40, Chapter 10.3] for more details on weak solutions to SDEs). By the Itô formula in [24, Corollary 2.6 point 2] it follows that on \mathcal{M} the dynamics of \tilde{Y}_t are

$$\begin{aligned} \tilde{Y}_t &= \sum_{i=1}^d (0, \eta_0) e_i + \sum_{i=1}^d \int_0^t \frac{\partial f_i}{\partial s}(s, \eta_s) e_i ds + \sum_{i,\alpha=1}^d \int_0^t (U_t e_{\alpha}) f_i(t, \eta_t) e_i dZ_s^{\alpha} \\ &\quad + \frac{1}{2} \sum_{i,\alpha,\beta=1}^d \int_0^t \operatorname{Hess}^{\nabla_t} f_i(U_t e_{\alpha}, U_t e_{\beta}) e_i d[Z^{\alpha}, Z^{\beta}]_s \\ &= \sum_{i=1}^d (0, \eta_0) e_i + \sum_{i=1}^d \int_0^t \frac{\partial f_i}{\partial s}(s, \eta_s) dse_i + \sum_{i,\alpha=1}^d \int_0^t (U_t e_{\alpha}) f_i(t, \eta_t) dZ_s^{\alpha} e_i \\ &\quad + \frac{1}{2} \sum_{i,\alpha,\beta=1}^d \int_0^t \left[\frac{\partial^2 f_i}{\partial x_{\alpha} \partial x_{\beta}}(t) \frac{\partial f_i}{\partial \gamma} \right] (U_t e_{\alpha}, U_t e_{\beta}) dx_{\alpha} \otimes dx_{\beta} d[Z^{\alpha}, Z^{\beta}]_s e_i \quad (\text{A.4}) \\ &= \sum_{i=1}^d (0, \eta_0) e_i + \left\{ \sum_{i=1}^d \int_0^t \frac{\partial f_i}{\partial s}(s, \eta_s) dse_i + \sum_{i,\alpha=1}^d \int_0^t (U_t e_{\alpha}) f_i(t, \eta_t) \langle c(s, \xi_s, Z_s), e_{\alpha} \rangle dt e_i \right. \\ &\quad \left. + \frac{1}{2} \sum_{i,\alpha,\beta,\gamma=1}^d \int_0^t \left[\frac{\partial^2 f_i}{\partial x_{\alpha} \partial x_{\beta}}(t) \frac{\partial f_i}{\partial \gamma} \right] (U_t e_{\alpha}, U_t e_{\beta}) (\alpha(t, \eta_t)^* \alpha(t, \eta_t))_{\alpha,\beta} e_i \right\} \\ &\quad + \sum_{i,\alpha=1}^d \int_0^t (U_t e_{\alpha}) f_i(t, \eta_t) \langle c(s, \xi_s, Z_s), e_{\alpha} \rangle dW_t^{\alpha} e_i \end{aligned}$$

This establishes the first point of Corollary 3.18.

Given the assumptions, the second point follows directly from the filtering equations in [11, Theorem 22.1.9]. \square

References

- [1] W. Ballmann. *Lectures on spaces of nonpositive curvature*, volume 25 of *DMV Seminar*. Birkhäuser Verlag, Basel, 1995. With an appendix by Misha Brin.
- [2] D. Bao, S.-S. Chern, and Z. Shen. *An introduction to Riemann-Finsler geometry*, volume 200 of *Graduate Texts in Mathematics*. Springer-Verlag, New York, 2000.
- [3] F. Barbaresco. Innovative tools for radar signal processing based on cartans geometry of spd matrices & information geometry. In *Radar Conference, 2008. RADAR'08. IEEE*, pages 1–6. IEEE, 2008.
- [4] M. J. Best. *Portfolio Optimization*. Chapman and Hall/CRC.
- [5] T. Björk and R. M. Gaspar. Interest rate theory and geometry. *Port. Math.*, 67(3):321–367, 2010.
- [6] S. Bonnabel and R. Sepulchre. Riemannian metric and geometric mean for positive semidefinite matrices of fixed rank. *SIAM Journal on Matrix Analysis and Applications*, 31(3):1055–1070, 2009.
- [7] A. Braides. A handbook of Γ -convergence. *Handbook of Differential Equations: stationary partial differential equations*, 3:101–213, 2006.
- [8] D. Brigo and F. Mercurio. *Interest rate models—theory and practice*. Springer Finance. Springer-Verlag, Berlin, second edition, 2006.
- [9] D. C. Brody and L. P. Hughston. Chaos and coherence: a new framework for interest-rate modelling. volume 460, pages 85–110, 2004. Stochastic analysis with applications to mathematical finance.
- [10] M. Bruveris, P. W. Michor, and D. Mumford. Geodesic completeness for Sobolev metrics on the space of immersed plane curves. volume 2, pages e19, 38, 2014.
- [11] S. N. Cohen and R. J. Elliott. *Stochastic calculus and applications*. Probability and its Applications. Springer, Cham, second edition, 2015.
- [12] E. De Giorgi and T. Franzoni. Su un tipo di convergenza variazionale. *Atti Accad. Naz. Lincei Rend. Cl. Sci. Fis. Mat. Natur. (8)*, 58(6):842–850, 1975.
- [13] F. X. Diebold and C. Li. Forecasting the term structure of government bond yields. *Journal of econometrics*, 130(2):337–364, 2006.
- [14] K. D. Elworthy. *Stochastic differential equations on manifolds*, volume 70 of *London Mathematical Society Lecture Note Series*. Cambridge University Press, Cambridge-New York, 1982.
- [15] K. D. Elworthy, Y. Le Jan, and X.-M. Li. *The geometry of filtering*. Frontiers in Mathematics. Birkhäuser Verlag, Basel, 2010.
- [16] D. Filipović. *Consistency problems for Heath-Jarrow-Morton interest rate models*, volume 1760 of *Lecture Notes in Mathematics*. Springer-Verlag, Berlin, 2001.

- [17] P. T. Fletcher. Geodesic regression and the theory of least squares on riemannian manifolds. *International journal of computer vision*, 105(2):171–185, 2013.
- [18] P. T. Fletcher, C. Lu, and S. Joshi. Statistics of shape via principal geodesic analysis on Lie groups. In *Computer Vision and Pattern Recognition, 2003. Proceedings. 2003 IEEE Computer Society Conference on*, volume 1, pages I–95. IEEE, 2003.
- [19] P. T. Fletcher, C. Lu, S. M. Pizer, and S. Joshi. Principal geodesic analysis for the study of nonlinear statistics of shape. *IEEE transactions on medical imaging*, 23(8):995–1005, 2004.
- [20] S. H. Friedberg, A. J. Insel, and L. E. Spence. *Linear algebra*. Prentice Hall, Inc., Upper Saddle River, NJ, third edition, 1997.
- [21] H. Geman and Y. F. Shih. Modeling commodity prices under the cev model. *The Journal of Alternative Investments*, 11(3):65–84, 2009.
- [22] A. A. Grigoryan. Stochastically complete manifolds. *Dokl. Akad. Nauk SSSR*, 290(3):534–537, 1986.
- [23] Y. Guan and J. G. Dy. Sparse probabilistic principal component analysis. In *Proceedings of AISTats*, volume 5, pages 185–192, 2009.
- [24] H. Guo, R. Philipowski, and A. Thalmaier. Martingales on manifolds with time-dependent connection. *J. Theoret. Probab.*, 28(3):1038–1062, 2015.
- [25] P. Hagan, A. Lesniewski, and D. Woodward. Probability distribution in the SABR model of stochastic volatility. In *Large deviations and asymptotic methods in finance*, volume 110 of *Springer Proc. Math. Stat.*, pages 1–35. Springer, 2015.
- [26] P. S. Hagan and D. E. Woodward. Equivalent Black volatilities. *Applied Mathematical Finance*, 6(3):147–157, 1999.
- [27] P. S. Hagan, D. Kumar, A. S. Lesniewski, and D. E. Woodward. Managing smile risk. *Willmott Magazine*, pages 84–108, September 2002.
- [28] C. Han and F. C. Park. A geometric GARCH framework for covariance dynamics. Available at SSRN: <https://ssrn.com/abstract=2827358>, 2016.
- [29] S. Hauberg, F. Lauze, and K. S. Pedersen. Unscented Kalman filtering on Riemannian manifolds. *J. Math. Imaging Vision*, 46(1):103–120, 2013.
- [30] D. Heath, R. Jarrow, and A. Morton. Bond pricing and the term structure of interest rates: A new methodology for contingent claims valuation. *Econometrica*, pages 77–105, 1992.
- [31] P. Henry-Labordère. *Analysis, geometry, and modeling in finance*. Chapman & Hall/CRC Financial Mathematics Series.
- [32] P. Henry-Labordère. A general asymptotic implied volatility for stochastic volatility models. arXiv, 2005. URL <http://arxiv.org/abs/cond-mat/0504317>.
- [33] S. L. Heston. A closed-form solution for options with stochastic volatility with applications to bond and currency options. *Review of Financial Studies*, 6(2):327–343, 1993.

[34] N. J. Higham and A. H. Al-Mohy. Computing matrix functions. *Acta Numer.*, 19:159–208, 2010.

[35] H. Hopf and W. Rinow. Über den begriff der vollständigen differentialgeometrischen fläche. *Commentarii Mathematici Helvetici*, 3(1):209–225, 1931.

[36] E. P. Hsu. *Stochastic analysis on manifolds*, volume 38 of *Graduate Studies in Mathematics*. American Mathematical Society, Providence, RI, 2002.

[37] J. Jost. *Riemannian geometry and geometric analysis*. Universitext. Springer, Heidelberg, sixth edition, 2011.

[38] T. Kailath. The divergence and Bhattacharyya distance measures in signal selection. *IEEE Transactions on Communication Technology*, 15(1):52–60, 1967.

[39] D. G. Kendall. Shape manifolds, Procrustean metrics, and complex projective spaces. *Bull. London Math. Soc.*, 16(2):81–121, 1984.

[40] G. J. Lord, C. E. Powell, and T. Shardlow. *An introduction to computational stochastic PDEs*. Cambridge Texts in Applied Mathematics. Cambridge University Press, New York, 2014.

[41] H. M. Markowitz. *Portfolio selection: efficient diversification of investments*, volume 16. Yale university press, 1968.

[42] P. W. Michor and D. Mumford. Riemannian geometries on spaces of plane curves. *J. Eur. Math. Soc. (JEMS)*, 8(1):1–48, 2006.

[43] M. Moakher and P. G. Batchelor. Symmetric positive-definite matrices: from geometry to applications and visualization. In *Visualization and processing of tensor fields*, Math. Vis., pages 285–298, 452. Springer, Berlin, 2006.

[44] M. Moakher and M. Zéraï. The riemannian geometry of the space of positive-definite matrices and its application to the regularization of positive-definite matrix-valued data. *Journal of Mathematical Imaging and Vision*, 40(2):171–187, 2011.

[45] J. Morgan and G. Tian. *Ricci flow and the Poincaré conjecture*, volume 3 of *Clay Mathematics Monographs*. American Mathematical Society, Providence, RI; Clay Mathematics Institute, Cambridge, MA, 2007.

[46] S. B. Morris. Book review: Hunter, JE, & Schmidt, FL (2004). Methods of Meta-Analysis: Correcting Error and Bias in Research Findings . Thousand Oaks, CA: Sage. *Organizational Research Methods*, 11(1):184–187, 2008.

[47] J. Nash. The imbedding problem for Riemannian manifolds. *Ann. of Math. (2)*, 63:20–63, 1956.

[48] X. Pennec, P. Fillard, and N. Ayache. A Riemannian framework for tensor computing. *International Journal of Computer Vision*, 66(1):41–66, 2006.

[49] M. K. Pitt. Smooth particle filters for likelihood evaluation and maximisation. Technical report, University of Warwick, Department of Economics, 2002.

[50] B. Rémillard. *Statistical methods for financial engineering*. CRC Press, Boca Raton, FL, 2013.

[51] S. Said and J. H. Manton. On filtering with observation in a manifold: reduction to a classical filtering problem. *SIAM J. Control Optim.*, 51(1):767–783, 2013.

[52] S. Said and J. H. Manton. Particle filtering with observations in a manifold. In *Acoustics, Speech and Signal Processing (ICASSP), 2015 IEEE International Conference on*, pages 5763–5767. IEEE, 2015.

[53] A. Sepp. Using SABR model to produce smooth local volatility surfaces. *Merrill Lynch, July*, 2007.

[54] S. T. Smith. Covariance, subspace, and intrinsic Cramér-Rao bounds. *IEEE Trans. Signal Process.*, 53(5):1610–1630, 2005.

[55] H. Snoussi. Particle filtering on Riemannian manifolds. Application to covariance matrices tracking. In *Matrix information geometry*, pages 427–449. Springer, Heidelberg, 2013.

[56] R. Tibshirani. Regression shrinkage and selection via the LASSO. *J. Roy. Statist. Soc. Ser. B*, 58(1):267–288, 1996.

[57] A. Tominaga. Extensions of Riemannian metrics. *J. Sci. Hiroshima Univ. Ser. A-I Math.*, 29:135–145, 1965.

[58] S. R. S. Varadhan. Large deviations and applications. *Exposition. Math.*, 3(3):251–272, 1985.

[59] S. Villa, L. Rosasco, S. Mosci, and A. Verri. Proximal methods for the latent group LASSO penalty. *Computational Optimization and Applications*, 58(2):381–407, 2014.

[60] F. W. Warner. *Foundations of differentiable manifolds and Lie groups*, volume 94 of *Graduate Texts in Mathematics*. Springer-Verlag, New York-Berlin, 1983. Corrected reprint of the 1971 edition.

[61] H. Whitney. Differentiable manifolds. *Ann. of Math. (2)*, 37(3):645–680, 1936.

[62] H. Zou and T. Hastie. Regularization and variable selection via the elastic net. *J. R. Stat. Soc. Ser. B Stat. Methodol.*, 67(2):301–320, 2005.

[63] H. Zou and H. H. Zhang. On the adaptive elastic-net with a diverging number of parameters. *Ann. Statist.*, 37(4):1733–1751, 2009.

[64] H. Zou, T. Hastie, and R. Tibshirani. Sparse principal component analysis. *J. Comput. Graph. Statist.*, 15(2):265–286, 2006.